Age-dependent deterioration in motor functions, circadian rhythm and sleep in *Drosophila* model of Amyotrophic Lateral Sclerosis 8

A Thesis

submitted to

Indian Institute of Science Education and Research Pune in partial fulfilment of the requirements for the BS-MS Dual Degree Programme

by

Vidyadheesh Kelkar

Indian Institute of Science Education and Research Pune

Dr. Homi Bhabha Road,

Pashan, Pune 411008, INDIA.

April, 2022

Supervisor: Dr. Girish Ratnaparkhi

Certificate

This is to certify that this dissertation entitled '*Age-dependent deterioration in motor functions, circadian rhythm and sleep in Drosophila model of Amyotrophic Lateral Sclerosis 8*' towards the partial fulfilment of the BS-MS dual degree programme at the Indian Institute of Science Education and Research, Pune represents study/work carried out by Vidyadheesh Kelkar at Indian Institute of Science Education and Research under the supervision of Dr. Girish Ratnaparkhi, Associate Professor, Department of Biology, during the academic year 2021-2022.

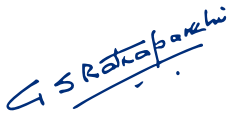

Dr. Girish Ratnaparkhi

Committee:
Dr. Girish Ratnaparkhi
Dr. Sutirth Dey

Vidyadheesh Kelkar
Date: 08/04/2022

This thesis is dedicated to my late grandfather
who nurtured my love for science and mathematics

Declaration

I hereby declare that the matter embodied in the report entitled '*Age-dependent deterioration in motor functions, circadian rhythm and sleep in Drosophila model of Amyotrophic Lateral Sclerosis 8*' are the results of the work carried out by me at the Department of Biology, Indian Institute of Science Education and Research, Pune, under the supervision of Dr. Girish Ratnaparkhi and the same has not been submitted elsewhere for any other degree

Vidyadheesh Kelkar

Date: 08/04/2022

Table of Contents

List of Figures

List of Tables

Acknowledgments

My 5-year journey at IISER has truly been a roller-coaster ride with a lot of ups and downs, twists and turns and full of great memories. A lot of people have supported me and helped me throughout this journey.

First and foremost, I express my gratitude to my supervisor Dr. Girish Ratnaparkhi for giving me the opportunity to work on this exciting project. He has been an ideal mentor and thesis supervisor always encouraging me to explore the depths of the problems on my own and offering insightful advice and helpful comments from time to time to guide me through the project. I have learned a lot about science and got a number of valuable life lessons in past three years working in his lab.

I would like to thank my project TAC member Dr. Sutirth Dey for his insights into the project. I thank Dr. Sheeba Vasu and Dr. Krishna Melanthur for their inputs and guidance.

I thank all present and past lab members for their helpful criticisms during lab meetings. I thank Lovleen, Kundan, Namrata, Sanhita and Subhrodeep for their amazing company and very refreshing distractions from the daily lab work.

I want to thank IISER Pune for this wonderful journey and DBT-INSPIRE scholarship for financial support.

Lastly, I thank my parents for always supporting me and being there for me. I thank my brother for always cheering me up with his humour. I thank all my friends who kept me sane during the fatiguing thesis work.

Abstract

Amyotrophic Lateral Sclerosis (ALS) is a fatal, motor neurodegenerative disease affecting thousands of people every year worldwide. ~50% of the ALS cases patients display behavioural changes, cognitive and executive dysfunction along with motor defects. In this study, I have used a *Drosophila* model of ALS to investigate the effects on behavioural patterns. The disease model is *Drosophila* variant with a point mutation in the *VAP* gene, where Proline in the 58th position is replaced by Serine (VAP^{P58S}), achieved by CRISPR-Cas9 genome editing.

Continuous monitoring of the daily activity of *VAP^{P58S}* flies using the *Drosophila* Activity Monitoring (DAM) system revealed that the flies exhibit progressive age-dependent motor defects and have a reduced lifespan. In addition to this, I found that these flies also show changes in their circadian rhythms and also sleep cycles. Mutant animals become arrhythmic with increasing age and lose the periodicity in their day-to-day motor activity. They have disturbed, fragmented sleep with number of 'short' sleep bouts increasing with age. This deterioration in lifespan, motor functions, circadian rhythm, and sleep is rescued by introducing a single copy of VAP^{WT} construct in the mutant flies.

My results underscore the utility of modelling human neurodegenerative disease in fly models. Our laboratory can now use the diverse genetic toolkit available in *Drosophila* to probe for molecular relationships between neurodegenerative disease and behaviour.

Chapter 1: Introduction

1.1 Amyotrophic Lateral Sclerosis:

Amyotrophic Lateral Sclerosis is a progressive neurodegenerative disorder. It is also known as Lou Gehrig's disease after the famous American baseball player who died from the disease. ALS was first described and diagnosed by French neurologist Jean-Martin Charcot in 1869 as a motor neuron disorder. His studies reported presence of lesions in the lateral column and the anterior horn of the spinal cord in the patients, which led to paralysis and muscle atrophy. Charcot coined the term Amyotrophic Lateral Sclerosis in his lectures in 1874 (Kumar et al., 2011). The term "amyotrophic" (from Greek, *A:* without; *myo:* muscle, *trophe:* nourishment) points to the lack of nourishment to and degeneration of muscles. The term "lateral" refers to the lateral region of the spinal cord, which is affected in ALS. Lastly, "sclerosis" (from Greek *sklerosis*: hardening) refers to the scarring of the brain and muscle tissues involved. ALS causes degeneration of upper motor neurons (UMN) of the motor cortex and Lower motor neurons (LMN) of the spinal cord and brainstem (Masrori & Van Damme, 2020). The degeneration leads to the loss of contact between the motor neurons and the postsynaptic muscles at the neuromuscular junction (NMJ), leading to muscle atrophy. This causes progressive motor defects in ALS patients. Earlier it was thought that ALS only affects the motor neurons. However recent studies have shown that ALS has a non-cell autonomous nature and affects the non-neuronal cells which contribute to motor neurodegeneration. In many cases, patients also suffer from extra-motor problems like behavioral changes, impairment in cognitive ability, executive dysfunction and language problems (Masrori & Van Damme, 2020).

The estimated incidence of ALS is 1.5-3 cases per 100,000 persons per year with a prevalence of 6-10 cases per 100,000 (Masrori & Van Damme, 2020; Talbott et al., 2016). The symptoms of ALS typically onset at the age of 55-60 years. It generally has a focal onset which subsequently spreads to other regions. Nearly ⅔ cases of ALS have a 'limb onset' marked by weakness in the limbs and cramping or twitching of the limb muscles. The weakness eventually leads to impairment of the muscles. The remaining ⅓ cases show a 'bulbar onset' of the disease, which causes dysarthria (difficulty in speaking) or dysphagia (difficulty in swallowing) (Wijesekera & Leigh,

2009). In some rare cases onset of the disease has respiratory components causing dyspnoea (Shortness of breath) and orthopnoea. As the disease progresses, muscle weakness and atrophy spread to other muscles in the body. Patients show signs of degeneration of both upper as well as lower motor neurons, which affects bulbar, thoracic, cervical and lumbar areas (Zarei et al., 2015). ALS is a fatal disease, with a typical life expectancy of 3-5 years post onset. A common reason for death in ALS is respiratory failure or choking due to the loss of control over diaphragm and thoracic muscles (Masrori & Van Damme, 2020; Wijesekera & Leigh, 2009; Zarei et al., 2015). As of today, there is no cure or effective treatment to stop the progression of ALS. Riluzole, a glutamate antagonist, is the only FDA approved drug that slightly prolongs the progression of the disease by some months. Edaravone, an antioxidant drug, is another medication proven to be effective in the early stages of ALS (Masrori & Van Damme, 2020; Jaiswal, 2019).

Most of the cases (~90%) of ALS are sporadic (sALS) and have no known cause or obvious genetic component associated with them. The remaining almost 10% of the cases have hereditary causes and familial origins and are known as familial ALS (fALS). Researchers have found more than 30 independent genetic loci associated with ALS. Mutations in these loci can potentially cause ALS. Both sporadic and familial ALS patients show mutations in one or more ALS associated genes. These mutations disrupt a variety of cellular functions, ultimately leading to motor neuron degeneration. Pathological studies of ALS patients have reported glutamate excitotoxicity, functional abnormalities in mitochondria, impaired axonal structure, protein aggregation, and elevated free-radical mediated oxidative stress (Wijesekera & Leigh, 2009; Zarei et al., 2015). These abnormalities and dysfunctions subsequently lead to neurodegeneration.

Although sporadic cases have no known cause and are considered non-genetic many sALS patients, like fALS cases, also show mutations in ALS associated genes. It is challenging to study the family history of sporadic cases because of the late onset. Researchers believe that some environmental factors may contribute to the sALS cases (Jaiswal, 2019). Some studies suggest that smoking or prolonged exposure to

smoking may be a risk factor for ALS (Armon, 2009). Exposure to chemicals like formaldehyde, pesticides, high concentrations of lead, and extremely low frequency electromagnetic radiation (Jaiswal, 2019; Weisskopf et al., 2009) also increases ALS susceptibility. Several case studies discuss about high physical activity being a risk factor for ALS (Jaiswal, 2019; Martin et al., 2017) In addition to these, having a glutamate (a neurotransmitter) rich diet is also thought to increase the risk of developing ALS (Jaiswal, 2019). Mutations in Superoxide Dismutase 1 (*SOD1*) gene and Chromosome 9 open reading frame 72 (*C9orf72*) has also been found in a significant fraction of sALS cases (Masrori & Van Damme, 2020; Wijesekera & Leigh, 2009; Zarei et al., 2015).

Some of the most common fALS loci, comprising almost 50% of the fALS cases, are Superoxide Dismutase 1 (*SOD1*) (*ALS1*), Chromosome 9 open reading frame 72 (*C9orf72*), TAR DNA binding protein 43 (*TDP-43*) (*ALS10*), and Fused in Sarcoma (*FUS*) (*ALS6*). The remaining ~25 loci constitute the other half of the fALS cases and have very low occurrence (Jaiswal, 2019; Mathis et al., 2019; Mejzini et al., 2019). The lack of enough patient samples has made studying the fundamental mechanism of ALS caused by mutations in these loci challenging. However, some of these rare loci have been very well characterized using model organisms like *C. elegans*, *Drosophila*, *Zebrafish*, and mice. These loci include genes like *VCP (ALS14), ubiquilin2 (ALS15), alsin (ALS2), senataxin (ALS4),* and *VAPB (ALS8)*. Most of the genetic loci follow an autosomal dominant, Mendelian inheritance. We, in our lab use a *Drosophila* model of ALS to study the effects of disease caused by a point mutation the VAP-33A (*Drosophila* homologue of VAPB) gene locus.

1.2 VAMP Associated Protein B (VAPB):

VAMP (Vesicle Associated Membrane Protein) Associated Protein B, or *VAPB*, is the 8th ALS loci to be discovered. Hence, the form of ALS associated with *VAPB* mutation is known as *ALS8*. So far, only two distinct missense mutations in *VAPB* (*T46I* and *P56S*) have been reported to be associated with fALS cases with, *P56S* being the most extensively studied of the two mutations. The mutation VAP^{P56S} was first found to be associated with familial ALS in a large white Brazilian family with 28 affected

patients across four generations (Nishimura et al., 2004; Nishimura et al., 2005). The same mutation has also been reported to be associated with Spinal Muscular Atrophy (SMA) (Marques et al., 2006).

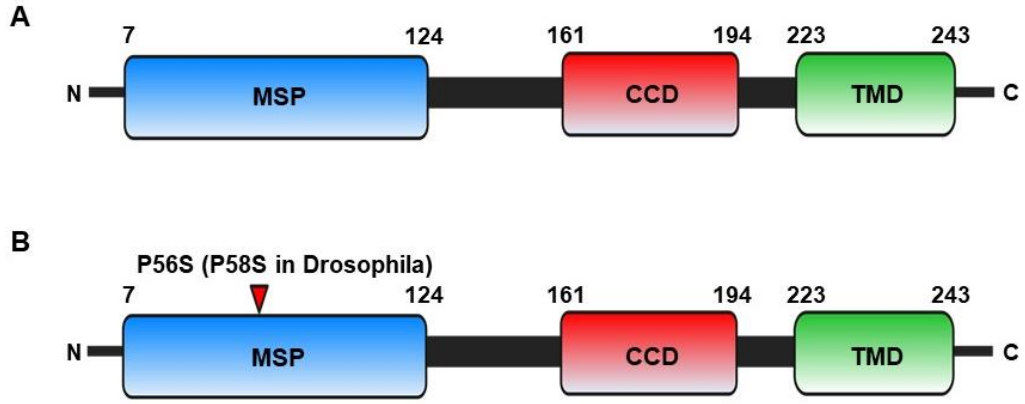

Figure 1.1 Structure of VAP
A) VAP has three domains, the N-terminal Major sperm protein (MSP) domain, the central coiled coiled domain (CCD) and the C-Terminal Transmembrane domain. **B)** The *P56S (P58S* in *Drosophila)* mutation is implicated in fALS cases and occurs in the MSP domain and disrupting the functions of VAP. Adapted from (James & Kehlenbach, 2021).

The gene VAPB codes for a highly conserved type-II ER membrane protein. The protein is composed of 3 domains, an N-Terminal Major Sperm Protein domain (MSP), the intermediate coiled-coil domain (CCD) and the C-terminal transmembrane domain (TMD) (James & Kehlenbach, 2021). VAP is situated on the ER membrane with the MSP domain extending into the cytoplasm instead of ER-lumen. The MSP domain mediates most of the VAPB functions and interacts with the other proteins. The CCD is also involved in binding to other proteins and also mediates oligomerization of VAPB. The TMD anchors the protein to the ER membrane. VAP is involved in various intracellular processes like membrane trafficking, microtubule organization, lipid transport and metabolism, ER-Golgi trafficking and Unfolded protein response (UPR) (Deivasigamani et al., 2014). It also maintains calcium homeostasis and have a role in bouton formation at neuromuscular junction (NMJ). (Kim et al., 2010; Pennetta et al. 2002) It interacts with the lipid transfer molecules at the ER-Golgi contact sites through an FFAT motif. It functions as a tethering molecule between ER and the other organelles. Most of the functions of *VAPB* are mediated by the MSP domain. The mutation at the 56th proline residue causes confirmational changes in MSP domain. This enhances the ability of VAP to oligomerize and form aggregates due to exposition

of hydrophobic entities (Kim et al., 2010). The MSP domain has been shown to be cleaved and secreted from ER membrane. The mutation *P56S* causes misfolding of MSP and hinders the cleavage disrupting downstream processes (Tsuda et al., 2008).

1.3 *Drosophila* Model of *ALS8*:

ALS is a very rare disease with an incidence rate of 1.5 - 3.00 cases per 100,000 persons per year (Masrori & Van Damme, 2020; Talbott et al., 2016). The lack of patient samples makes it difficult to study the fundamental mechanisms involved in the disease. The rare ALS loci like *VCP, VAPB, alsin, ubiquilin2* have been characterized with the help of model organisms. Expression of the ALS-associated mutations in a model organism has not only helped in understanding the disease mechanisms but also provided an insight into therapeutic targets for the treatment of ALS. Over the years organisms such as yeast, nematode worm *C. elegans, Zebrafish*, fruit flies and mice have been used as model organisms to study molecular and genetic mechanisms of ALS. *Drosophila melanogaster* because of its short life span, ease of handling, simplicity of genetics, advanced genetic tools and about 60% homology with humans has been used extensively as a model organism for many neurodegenerative disease studies including ALS. Some of the commonly used phenotypes to study motor neurodegenerative diseases in *Drosophila* include motor defects in larvae and adults, survival assays, protein aggregates, neuronal morphology, brain imaging and immunohistochemistry to observe cellular defects.

We use a *Drosophila melanogaster* model of *ALS8* i.e., we generate a missense Proline to Serine mutation at the 58th residue (P56S in Humans) in the fly *VAP33A* gene. Generation of this mutant *VAP33A(P58S)* has been shown to cause ALS-like symptoms in *Drosophila.*

We had previously used a null-rescue model to study the effects of ALS in the flies. The original genetic background of this null line was a deletion on the X-Chromosome caused by an imprecise P-element excision causing a deletion of 1kb in the VAP-33A gene. This gene variant encodes a truncated protein of around 20Kda producing a hypomorphic allele of VAP (∆166) (Moustaqim-Barrett et al., 2014) We introduced an extra copy of VAP^{WT} & VAP^{P58S} under a genomic promoter on the 3rd chromosome in these null lines separately generating two distinct fly lines, ∆VAP; *g*VAP^{WT} and ∆VAP;

*g*VAP^{P58S}. The small ‘g’ indicates genomic inserts (in the third chromosome), driven by the *VAP33A* promoter. These lines have been characterized and studied thoroughly (Moustaqim-Barrette et al., 2014; Tendulkar et al. 2022)

For the purpose of this study, I have used a CRISPR-edited *Drosophila* line, generated in our laboratory, with a point mutation in the *VAP33A* (hereafter referred to as VAP^{P58S}) locus. The main difference in the Null-Rescue line and the CRISPR edited line is that the CRISPR line, the gene is in its normal genomic location on the X-Chromosome instead, and the mutation (Proline to Serine codon change) is within the *VAP* locus. The CRISPR line mimics a natural mutation and has the added advantage that both males and females can be studied (as opposed to the null-rescue line). Another advantage of the CRISPR *VAP^{P58S}* line is the availability of the 3rd Chromosome for experimental manipulation.

The previous studies in our lab using the CRISPR line have shown that the VAP^{P58S} flies exhibit survival defects with a median lifespan of around 23 days. The climbing assays reported that these flies also exhibit progressive motor defects and lose walking and flying abilities as they age (as the disease progresses). The brain imaging studies have showed that the flies show presence of VAP-positive brain aggregates which are rescued by a single dose of wild-type VAP. The data from neuromuscular junction (NMJ) imaging suggests that the VAP^{P58S} flies have defects in NMJ morphology. Impairment in the function of VAPB affects the neuronal bouton numbers and size.

It is evident from the previous studies in our lab that the flies carrying the VAP^{P58S} mutation show progressive motor neurodegeneration. Through various studies worldwide, ALS has also been reported to have a non-cell autonomous effect affecting the non-neuronal cells like dendritic cells, astrocytes, and glia. In more than 50% of cases patients have also shown to exhibit extra-motor defects and behavioral changes (Masrori & Van Damme, 2020). Therefore, we wanted to further characterize the age-dependent neurodegeneration in ALS to check how this affects motor as well as extra-motor functions in *Drosophila.* To further elucidate the effects, we have used the

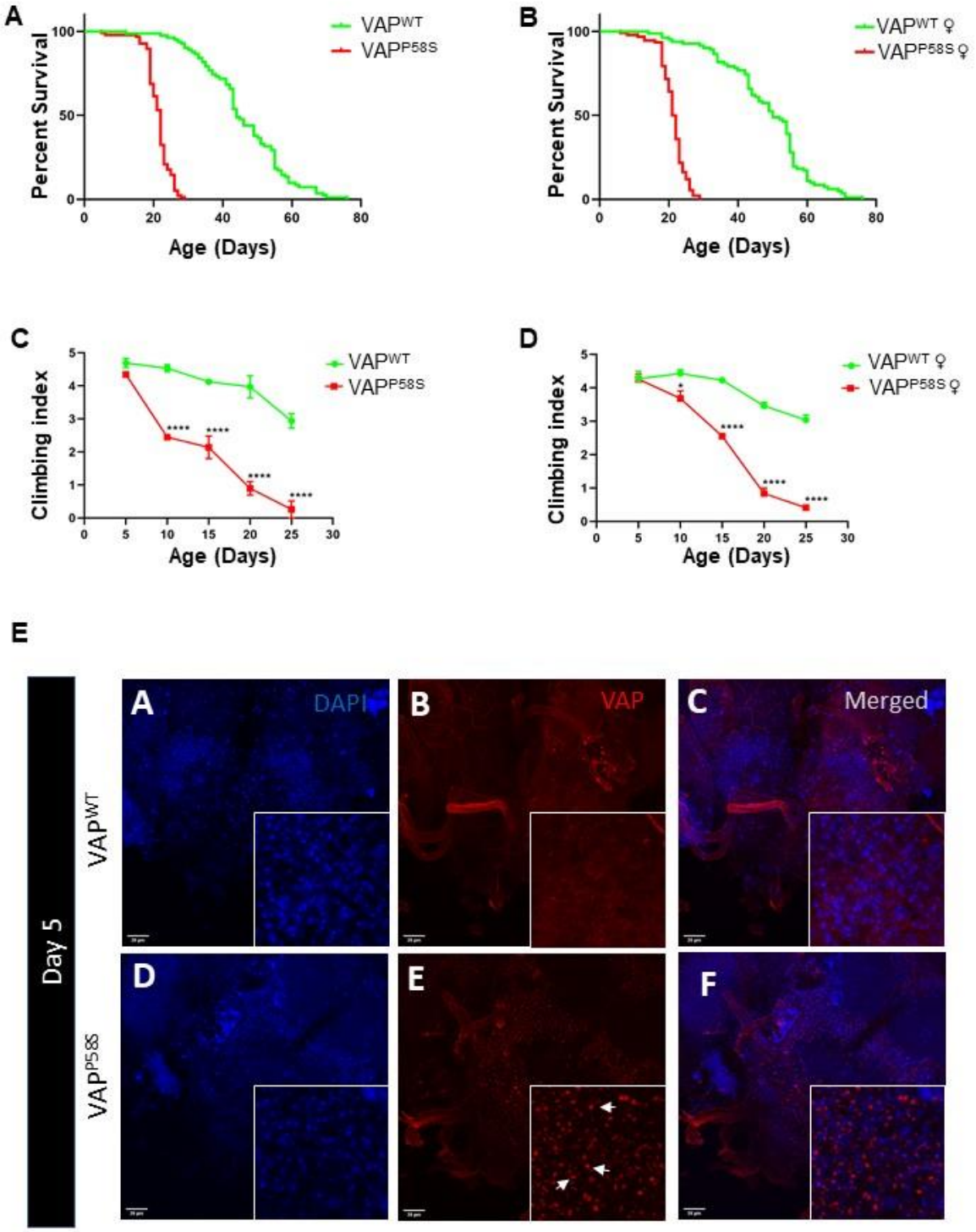

Figure 1.2. Characterization of CRISPR model.
A),B) Survival assays for male and female VAP^{P58S} flies respectively. The VAP^{P58S} flies show survival defects and have a reduced median lifespan of ~23 days. **C), D)** Results from the climbing assays report progressive motor defects in VAP^{P58S} male and female flies. **E)** The VAP^{P58S} CRISPR mutants show presence of VAP positive protein aggregates. *Unpublished data from the thesis of Aparna Thulasidharan and Namrata Kulkarni.*

Drosophila Activity Monitoring (DAM) system, developed by Trikinetics which has been proven to be useful for behavioral studies in drosophila. I standardized a DAM system protocol for conducting motor assays on *Drosophila*. I performed continuous activity monitoring and locomotor activity assays of the *ALS8* model flies to check for the effects of neurodegeneration on the overall activity and behavioral patterns like circadian rhythm and sleep-wake cycles in *Drosophila.*

1.4 Drosophila Activity Monitoring (DAM) System:

The Drosophila Activity Monitoring (DAM) system developed by Trikinetics is an automated device, that uses infrared beams to detect and quantify the movement of drosophila over time. The system consists of a host computer (Mac or Windows) along with a set of activity monitors and a central power supply unit. The activity monitors are connected to the power supply interface unit (PSIU) through telephone cables.

The monitors are housed inside an incubator to provide stable temperature and light conditions throughout the duration of the experiment. The PSIU collects the data from the monitors at regular intervals and sends it to the host computer via a USB port. Using 5-way splitters and couplers, one PSIU can host up to 120 monitors at a time with each monitor carrying 32 activity tubes. The system allows individual as well as population behavior monitoring and has been proven very effective in behavioral studies. The figure 1.3. shows a general schematic of the DAM system.

The system uses transparent glass tubes to house the flies. These tubes are then loaded onto the activity monitors which use infrared beams to measure the activity of the flies over time. The tubes are adjusted in such a way that the beam passes through the middle of the tubes and as the fly moves back and forth inside the tube the beam gets cut. The system quantifies the activity based on the number of times the infrared beam gets cut in a given period of time. The system operates continuously over a period of days or weeks and captures the daily locomotor activity of the flies. The tubes can be filled with food to keep the flies from starving without interrupting the system.

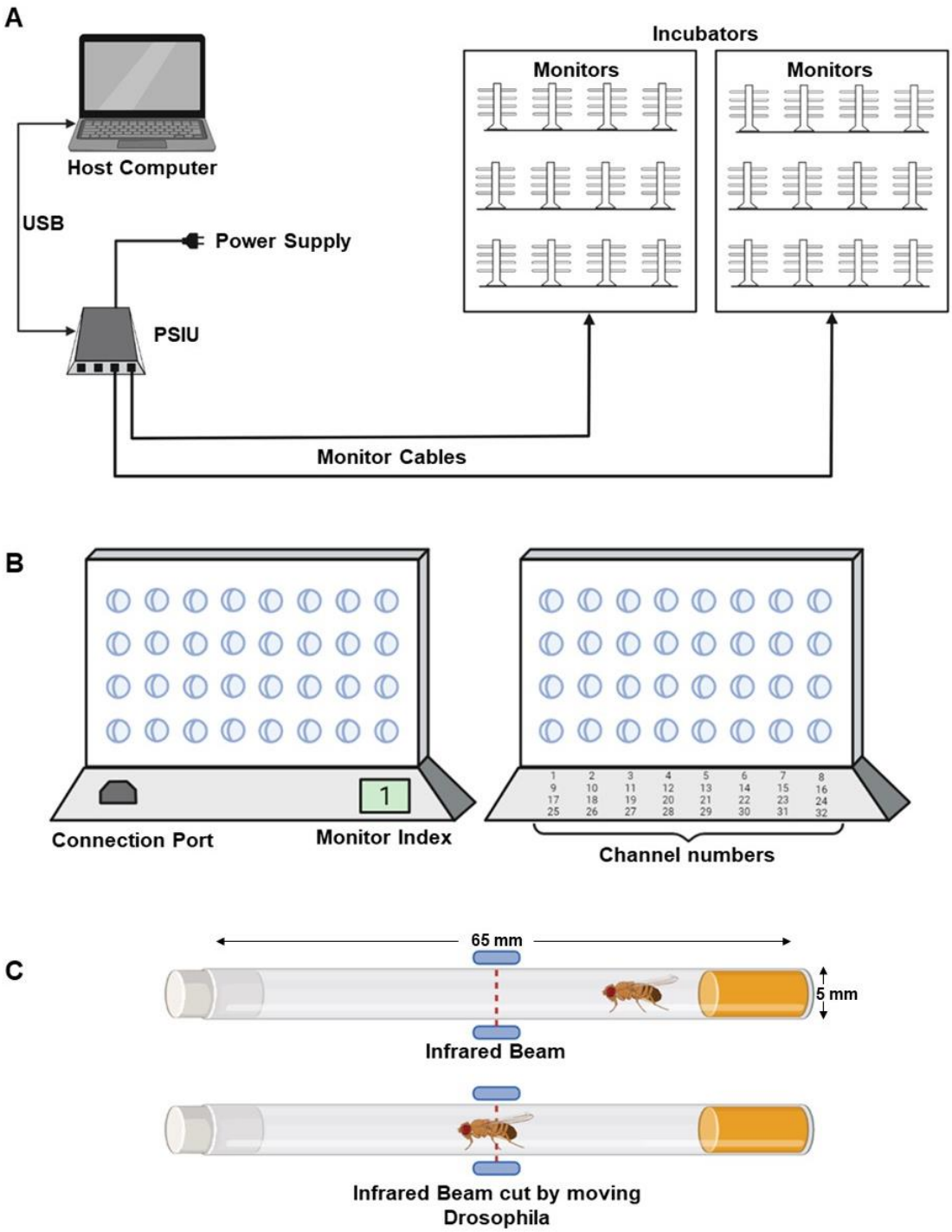

Figure 1.3. The Drosophila Activity Monitoring System.
A) The general schema of DAM system and how different components are connected together. **B)** The DAM system activity monitor (front and back). Each monitor can house 32 activity tubes. Each monitor is indexed and is connected to the PSIU via a telephone cable. **C)** The activity tubes housing the flies. The infrared beam goes through the middle of the tube when it is inserted into the monitor holes. The beam gets cut as the fly moves inside the tube.

The Drosophila activity monitoring system provides a robust, repeatable, and easy means to quantify the daily activity of flies. These daily activity measures can then be used to further calculate different behavioral parameters like Circadian Rhythm, Sleep-Wake cycle, social interaction, Population behavior, phototaxis, geotaxis, etc. It is also compatible with very large experiments as one PSIU can collect data for ~3000 individuals. The infrared beam used for detection allows the system to be operated in light or dark, in any orientation and temperature.

Using the robust and efficient way of monitoring the daily activity of *Drosophila* provided by the DAM system I was able to characterize the effects of the neurodegeneration in *ALS8* on the overall fly activity and behavior. The DAM system provided us with a better alternative to conduct motor assays on *Drosophila* over the conventional climbing assays. The study revealed that the drosophila carrying the VAP^{P58S} mutation show progressive motor and survival defects. These mutant flies have a diminished activity and a shorter lifespan as compared to the VAP^{WT} flies. The circadian rhythm of the VAP^{P58S} mutant flies is lost as they age. The old (~20 days of age) VAP^{P58S} flies are arrhythmic and show no periodicity in their day-to-day activity. The mutation also disrupts the Sleep wake cycle of the flies. These behavioral changes are rescued by introducing a single copy of wildtype VAP in the VAP^{P58S} mutant flies.

Chapter 2: Materials and Methods

2.1 *Drosophila* Husbandry:

The flies used for the experimental purposes were entrained to a 12:12 hr Light/Dark cycle. The incubators were maintained at a temperature of 25°C under standard laboratory conditions. Flies were raised on a standard cornmeal diet. All the crosses were set up at 25°C. The Canton-S and w^{1118} (white eyed) flies were used as wild-type control. The CRISPR edited VAP^{P58S} mutant line along with a control VAP^{WT} were used for the experiments. The following table shows the detailed description of the fly lines involved.

Table 2.1. Description of the fly lines used.

Fly Line	Full Genotype	Details
Canton-S	*+;+;+*	Wildtype Control
w^{1118}		Wildtype Control
VAP^{P58S}	VAP^{P58S}*/FM7a; +; +*	A CRISPR edited Drosophila model of ALS8 (Primary test subject)
VAP^{WT}	VAP^{WT}*/FM7a; +; +*	Wildtype Control
ΔVAP; gVAP^{P58S}	*Δ166/FM7a; +; genomic* VAP^{P58S}*/TM3Tb*	Null-Rescue system
ΔVAP; gVAP^{WT}	*Δ166/FM7a; +; genomic* VAP^{WT}*/TM3Tb*	Null-Rescue system

2.2 Activity Assay:

I carried out locomotor activity assays using the DAM2 system by Trikinetics to monitor the effect of neurodegeneration due to the ALS mutation. The data obtained from the activity assays was then further used for analysing the different behavioral parameters like circadian rhythm, Sleep-wake cycle and overall activity of the flies. We continuously monitored the flies over a span of ~20 days under stable laboratory conditions.

The fly lines were maintained at 25°C with a 12:12h LD cycle. The newly eclosed flies were transferred to a separate bottle with fresh media. The flies were allowed to mate before sorting the male and female flies into individual vials. The male and female flies were separated on the 2nd day after eclosion. 32 age matched male flies per genotype were collected for the experiments since one activity monitor can house up to 32 individual tubes. 3-day old male flies were loaded into the DAM system activity tubes (65X5 mm Pyrex glass tubes) filled with standard, 3% cornmeal fly media at one end. The food end was sealed off using parafilm to keep the food from drying out quickly. The other end was plugged using a cotton plug. The flies were given 24hrs to acclimate to the new environment before starting the continuous monitoring. The activity of the flies was monitored 4th day onwards starting at 12:00 am. The incubator temperature was maintained at 25°C, with a 12h:12h Light-Dark cycle for the entire duration of each experiment. The lights were programmed to turn on at 7:00 am in the morning and turn off at 7:00 pm. Flies were transferred to new activity tubes with fresh media every 4th day to keep them from starving and to keep the continuous monitoring unhindered. The flies were monitored till the age of 22-23 days by which time more than half of the ALS mutant flies are dead.

The reading interval for the activity counts was set to be 1 minute in the *DAMSystem311* software for ease of further calculations. The data obtained from the activity assays was then used for circadian rhythm and sleep analysis and other activity measurements.

2.2.1 Activity Tubes Preparation:

The activity tubes used for the DAM system assays were filled with standard cornmeal media to keep the fly from starving. To fill the tubes with food, 30ml of liquified media was taken into a 100ml beaker. ~40 activity tubes were tied in a bunch using a rubber band and were dipped in the media together. The beakers were kept into freezer at 4°C temperature for 2hours to solidify the media. After the media was set, the tubes were gently pulled out with media inside them. The food end was sealed off using parafilm to keep it from drying. The tubes were kept at 4°C till the time of experiment.

2.2.2 Activity Tube Recycling:

The activity tubes were changed every 4th day to provide the flies with fresh food. The used tubes were recycled after thorough cleaning. To wash out the old media the tubes were kept in boiling water. The empty tubes were then soaked in warm soap water for 15 minutes. The tubes were washed and dried completely and were then autoclaved before using them again.

2.3 Calculation of Circadian Rhythm and Sleep Data:

The data obtained from the DAM system was analyzed further to measure the different behavioral patterns like circadian rhythm, locomotor activity, and sleep/wake cycle of the ALS8 model flies. We used the freely available R-based open-source programs *RhythmicAlly* (Lakshman & Vasu, 2019) and *VANESSA* (Ghosh & Vasu, 2022) to analyze the circadian and sleep patterns of the flies respectively. The circadian and sleep parameters obtained from the programs were then plotted and analyzed using GraphPad Prism9 graphing software and Excel.

The raw data files obtained from the *DAMSystem311* software were first processed using the *DAMFileScan113.* The 1-minute bin data was summed into 30-minute bins and was clubbed into an overlapping set of 3 days each for Circadian rhythm analysis. For example, Set-1 consisted of activity readings from days 4,5 & 6 while Set-2 was comprised of days 5,6,7, and so on. 1 day was considered as a 24-hr window starting from 12:00 am. (See Figure 2.1). On the other hand, for sleep analysis, data was compiled in 1-minute bins starting from 7:00 am (ZT0) on the first day of monitoring to 7:00 am of the last day of assay. (See Figure 2.1 B) These sets were then used to

calculate daily activity profiles and circadian & sleep parameters through *RhythmicAlly* and *VANESSA* respectively.

2.3.1 Circadian Rhythm: *RhythmicAlly* uses the text files obtained from the *DAMFileScan113* to calculate the circadian rhythm periods and generate actograms and plots. The program generates an average 24hr activity profile for each monitor channel (i.e., individual flies) using the activity counts per bin per day. For example, loading the Set1 into the program will average the activity over the 3 days in that set i.e., 4th, 5^{th,} and 6th. This average can be effectively used as the average activity for Day 5 for each fly. These average activity profiles were then used to plot the circadian rhythms. I averaged this average individual fly activity over all the individuals (32 flies per run) to obtain a 24hr average activity profile for each day. These profiles were then plotted using the software GraphPad Prism9 to visualize the circadian rhythm. The actograms encompassing the entire duration of the experiment were plotted using *MS Excel.* This was followed for each activity assay.

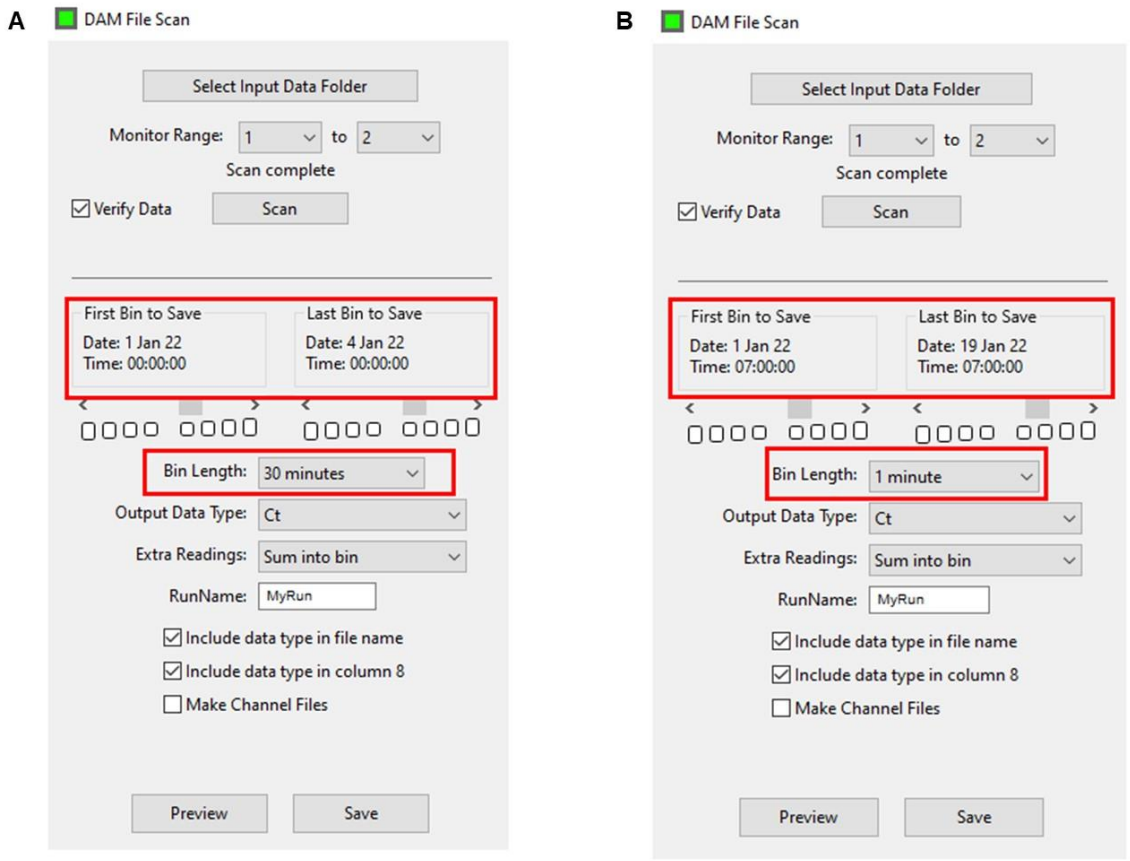

Figure 2.1 Processing of Raw Monitor files for further analysis by *DAMFileScan* Software. A) Binning of the data for circadian analysis. Each processed file contained activity readings for 3 consecutive days summed into 30-min bins. Summing started from 00:00:00 hrs of first day and

ended on 00:00:00 hrs of 4th day, encompassing 3 whole 24hr days. **B)** For sleep data the raw files were summed into 1-min bins, starting from 7:00:00 hrs of day 1 of the experiment till the last day of the experiment.

2.3.2 Sleep Analysis: The sleep patterns of *Drosophila* were analysed using the R-based open-source program VANESSA. The program provides a very efficient platform to calculate various sleep and circadian parameters. VANESSA uses the text files obtained from the *DAMFileScan113* software and a formatted Metadata file to calculate sleep parameters for specified day or duration. The program generates graphs depicting different sleep parameters like sleep profile, total sleep, number of sleep episodes, length of sleep bouts and latency for each day. The program also records the Light and Dark condition data separately.

The data files obtained from the program were used to plot the graphs for each sleep parameter using GraphPad Prism9 software. The sleep parameters were first averaged over all the individuals to obtain the mean value for each day. These means along with SEM were then used to compare the different sleep parameters between VAP^{P58S} and VAP^{WT} flies. The graphs were analyzed using 2-way ANOVA test with multiple comparisons with the genotype and age (days) being the two categorical variables for the different sleep parameters. The significance of the difference in means was tested using Tukey's test. The analysis was done using the GraphPad Prism9 software.

2.4 Activity Comparisons:

The ALS flies show deterioration in motor functions overtime. In the early stages, the wildtype, as well as mutant flies, show distinct morning and evening activity peaks. The flies exhibit a daily rhythm with a single prominent maximum at the time of L-D transition. I considered this Maximum Activity per day as a measure to visualize the progressive deterioration in the motor activity of the flies and compare the daily activity of different fly lines. The daily activity data obtained was plotted using the GraphPad Prism9 software. The data was fit to an equation using Simple linear regression to observe the trends in the motor activity overtime. The regression lines were compared pairwise to check whether the lines were different from each other significantly.

2.5 Survival Assays:

The survival of he flies was monitored during the activity assays. The RhythmicAlly and VANESSA programs identify the dead flies and omits them from the calculations. The actograms generated by these programs were used to keep track of the survival of the flies. The data was then plotted as Kaplan-Meier curves using GraphPad Prism9 software.

Chapter 3: Results

3.1 *VAP^{P58S}* flies show progressive motor defects.

The previous studies in our lab using the Null-Rescue and CRISPR edited *ALS8* fly models have shown that the flies carrying the VAP^{P58S} mutation exhibit progressive motor defects. The deterioration in the motor functions was characterized using standard climbing assays. These are startle-induced negative geotaxis assays and measure the climbing ability of the flies inside a long cylindrical column. Though the assay can successfully detect and differentiate between the good and bad climbers it is based on the response of the flies to the startle (or external stimuli). The sleeping flies have an increased arousal threshold (Beckwith & French, 2019) and decreased responsiveness to outside stimuli (Kume et al., 2005). This characteristic of sleep may hinder with the climbing assays. On the other hand, the DAM system provides a more stable and controlled environment to carry out motor assays. It provides a way to continuously monitor the fly activity over a long period of time. I performed continuous activity assays of the flies using the DAM system over a period of 20 days. I used the data obtained from these assays to quantify and compare the motor activity of flies. (See Materials & Methods).

As the Figure 3.1 depicts, the VAP^{P58S} flies have an overall diminished activity as compared to the VAP^{WT} flies of same age. The activity of VAP^{WT} flies is comparable to that of the wildtype control w^{1118} & *CS* flies. The VAP^{P58S} flies show a steady decrease in their daily activity as they age. There is approximately a 2.5-fold change in the activity of VAP^{P58S} flies going from 5th day to 20th day of age. Based on the bin size (30-min) we can clearly see that by the age of 20 days the VAP^{P58S} flies exhibit very low, nearly negligible activity with not more than 1 activity count per minute. On the other hand, the VAP^{WT} flies show a very small dip in the activity by the time they are 20 days old. The VAP^{WT} flies show a ~2-fold higher activity as compared to the VAP^{P58S} mutant flies at the age of 20 days. In addition to the motor defects the VAP^{P58S} flies also exhibit survival defects. More than 50% of the flies are dead by the age of 20 days.

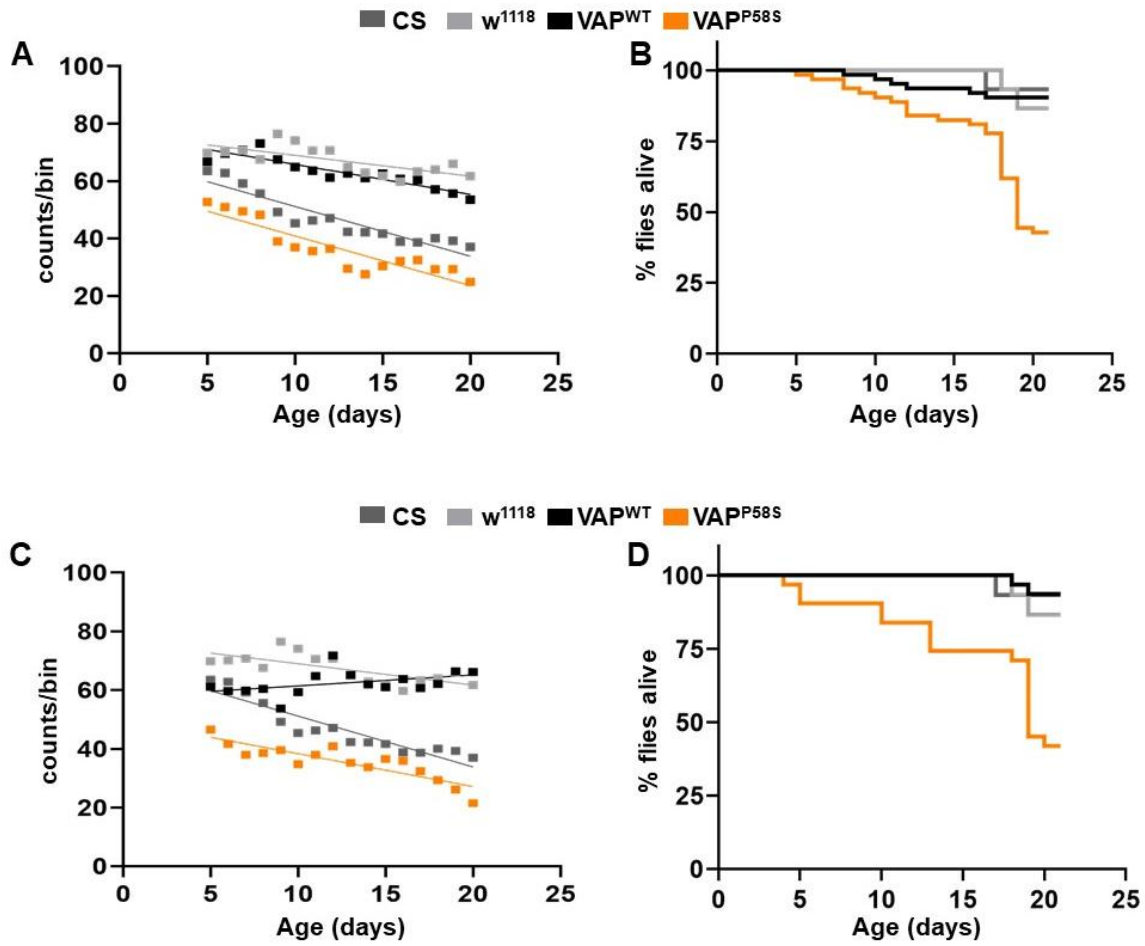

Figure 3.1. VAP^{P58S} flies exhibit survival and motor defects.

A) Motor Activity plots for *w^{1118}* (wildtype control; light grey curve; n=32), *CS* (wildtype control; dark grey curve; n=32), *VAP^{WT}* (control; black curve; n=32, N=2), *VAP^{P58S}* (orange curve; n=32; N=2) male flies. **B)** The survival curves for the same genotypes. *VAP^{P58S}* flies have a median lifespan of 19 days. Curve comparison was done using log-rank (Mantel-Cox) test. Curves are significantly different with an overall **p-value of *p*=0.0047**. **C)** The motor activity plots for female *VAP^{WT}* (black curve; n=32) and *VAP^{P58S}* (orange curve; n=32) flies along with *CS* and *w^{1118}* wildtype controls. **D)** Survival curves for female flies. Curve comparison was done using log-rank (Mantel-Cox) test. Curves are significantly different with an overall **p-value of *p*=0.000037.**

The Panel C shows the activity data for the female flies. The female flies show a similar trend in the activity as the male flies. The female VAP^{P58S} flies show similar decrease in the daily activity with age and show a ~3-fold difference in activity on day 20 as compared to the VAP^{WT} females of same age. The female flies show a greater variability in the daily activity measures as compared to the male flies which can be associated to the egg laying in the females.

The results obtained from the activity assays using the DAM system are at par with the previously conducted studies on the *ALS8* model flies in our lab. The neurodegeneration in the ALS flies affects their overall activity and have a severe effect on their survival. The decrease in daily activity also results in changes in the behavioral patterns of the flies.

3.2 The mutant VAP^{P58S} flies lose circadian rhythm over time and become arrhythmic.

The Circadian rhythm is a natural cycle followed by the physical, mental, and behavioral changes in an organism. These are endogenous processes that are entrained by the environment around the organism. The circadian rhythms respond primarily to light and follow a roughly 24-hour cycle. This can affect sleep, body temperatures, hormone levels, appetite, and other bodily functions. The circadian rhythms coordinate a number of biological processes in animals, plants, and microbes. These rhythms in different processes are regulated by the biological clocks present in different tissues. These clocks are small protein molecules that temporally regulate these processes. A group of neurons in the brain, called the master clock coordinates the biological clocks in the body and keeps them in sync. [22]

The circadian rhythm has been very well studied using *Drosophila melanogaster.* The discovery of the *clock genes* in *Drosophila* was a stepping stone in understanding the functions of biological clocks (Tataroglu & Emery, 2014). The studies have shown that the circadian rhythm in *drosophila* also follows a 24hr cycle of rest and activity. The flies display an increase in locomotor activity at dawn and dusk. Under laboratory conditions, the flies are entrained to a 12:12 hour Light-Dark cycle. They show a similar circadian rhythm pattern with activity peaks in anticipation of light to dark and dark to light transitions. Since the mutation in VAPB affects the motor neuronal and NMJ morphology resulting in loss of motor function, we wanted to examine whether this decrease in locomotor activity affects the rhythmicity of these flies. We conducted locomotor activity assays and continuous monitoring of the VAP^{P58S} mutant flies using the DAM system.

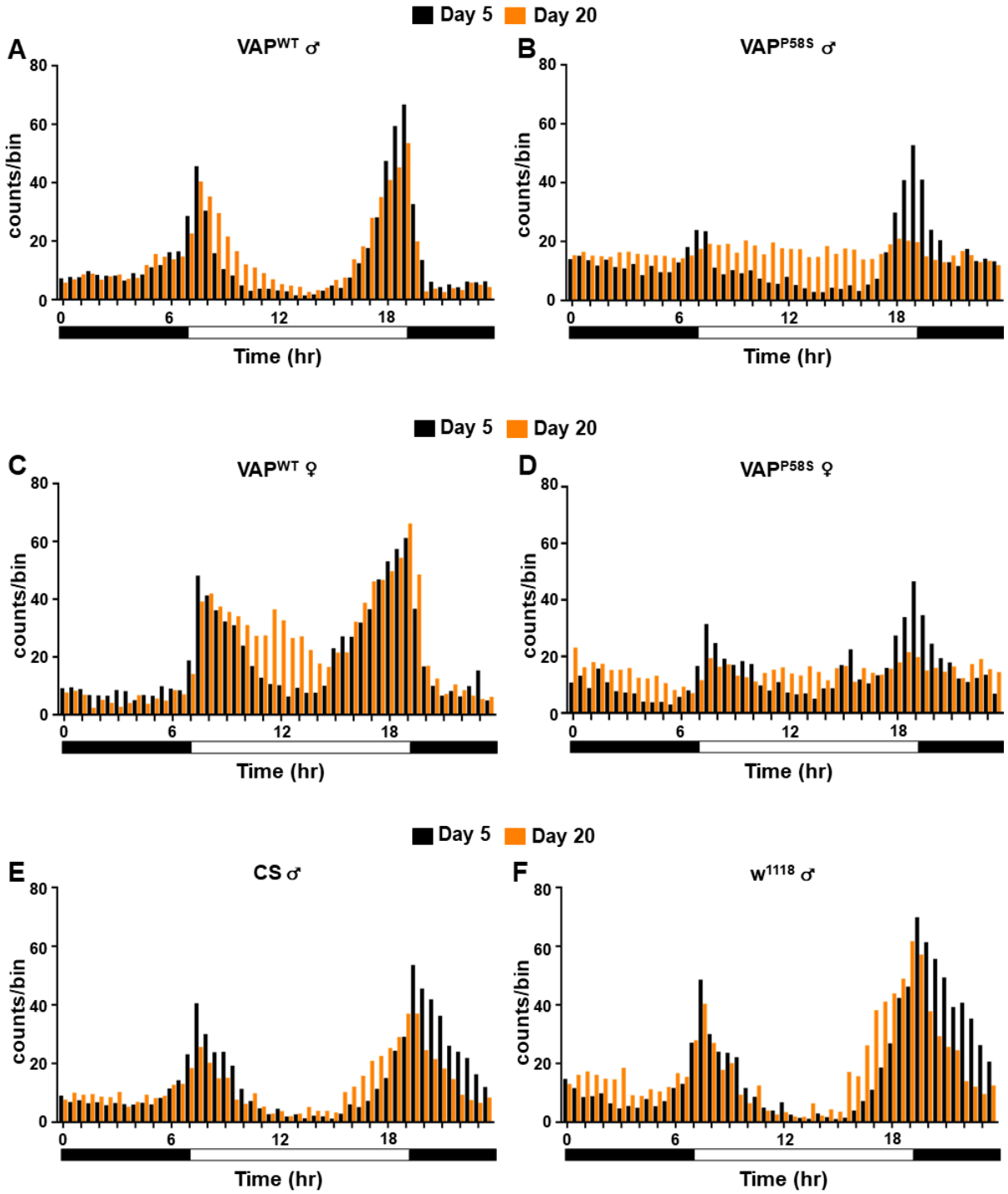

Figure 3.2. VAP^{P58S} flies lose circadian rhythm.
The y-axis represents the activity counts per 30-minute bins. The x-axis represents the time of the day with 0 being 00:00:00 hrs (12:00 am). The graphs compare the circadian rhythms on day 5 and day 20 for each genotype. The bar under the x-axis shows the light-dark conditions inside the incubator. The lights are turned on at 7:00 am and are turned off at 7:00pm.
A) VAP^{WT} male flies. (n=32, N=2) **B)** VAP^{P58S} male flies. (n=32, N=2) **C)** VAP^{WT} female flies. (n=32, N=1) **D)** VAP^{P58S} female flies. (n=32, N=1) **E)** *CS* male flies. (n=32, N=1) **F)** w^{1118} male flies (n=32, N=1).

The locomotor activity assays for *CS* and w^{1118} flies reported a normal circadian rhythm pattern with two distinct activity peaks. (Figure 3.2. E&F) The assays were then carried out using the VAP^{P58} flies with the VAP^{WT} line serving as the control. The VAP^{WT} flies exhibited a normal circadian rhythm similar to that of *CS* and w^{1118} flies. VAP^{P58S} mutants, however, displayed a progressive loss in the rhythmicity. Though the young mutant flies, ~5-7 days old demonstrate a normal circadian rhythm, the morning activity peak of these flies is shorter as compared to the VAP^{WT}. The mutant flies have slightly decreased activity in the morning period. Eventually, mutant flies show a decrease in the evening activity peak. As the flies age, they become arrhythmic and show a constant very low activity throughout the day. The Circadian data for the VAP^{WT} & VAP^{P58S} flies is depicted in figure 3.2. The VAP^{P58S} flies lose their motor activity and become arrhythmic by the age of 20 days. They exhibit a very low, nearly negligible activity with ~0.66 counts/min and eventually die by the age of 23-24 days as mentioned before.

The actograms encompassing the circadian rhythms for each day of the experiment given in the figure 3.3. clearly shows that the VAP^{WT} flies exhibit no changes in the rhythm over the span of the assay. On the other hand, the VAP^{P58S} mutants show a stable decrease in the activity after the $7^{th}/8^{th}$ day and lose the rhythmicity completely in the later stages. The morning as well as evening activity is diminished and the flies lose the periodicity in the daily activity.

The female VAP^{P58S} mutant flies also display a similar pattern in the circadian rhythm deterioration. (Figure 3.2. C&D) The female mutant flies become arrhythmic by the age of 20 days with a basal very low activity throughout the day. The VAP^{WT} female flies show no reduction in the activity counts at the morning and evening peaks. However, there is a significant increase in the activity in the afternoon for the female flies with the increase in age. Both the male and female VAP^{P58S} mutant flies exhibit circadian rhythm defects and become arrhythmic with age.

It is evident from the circadian analysis that the ALS mutant flies lose circadian rhythm and periodicity. Next, we wanted to check how the ALS affects the sleep-wake cycle in *Drosophila* and whether the sleep behavior of flies also changes.

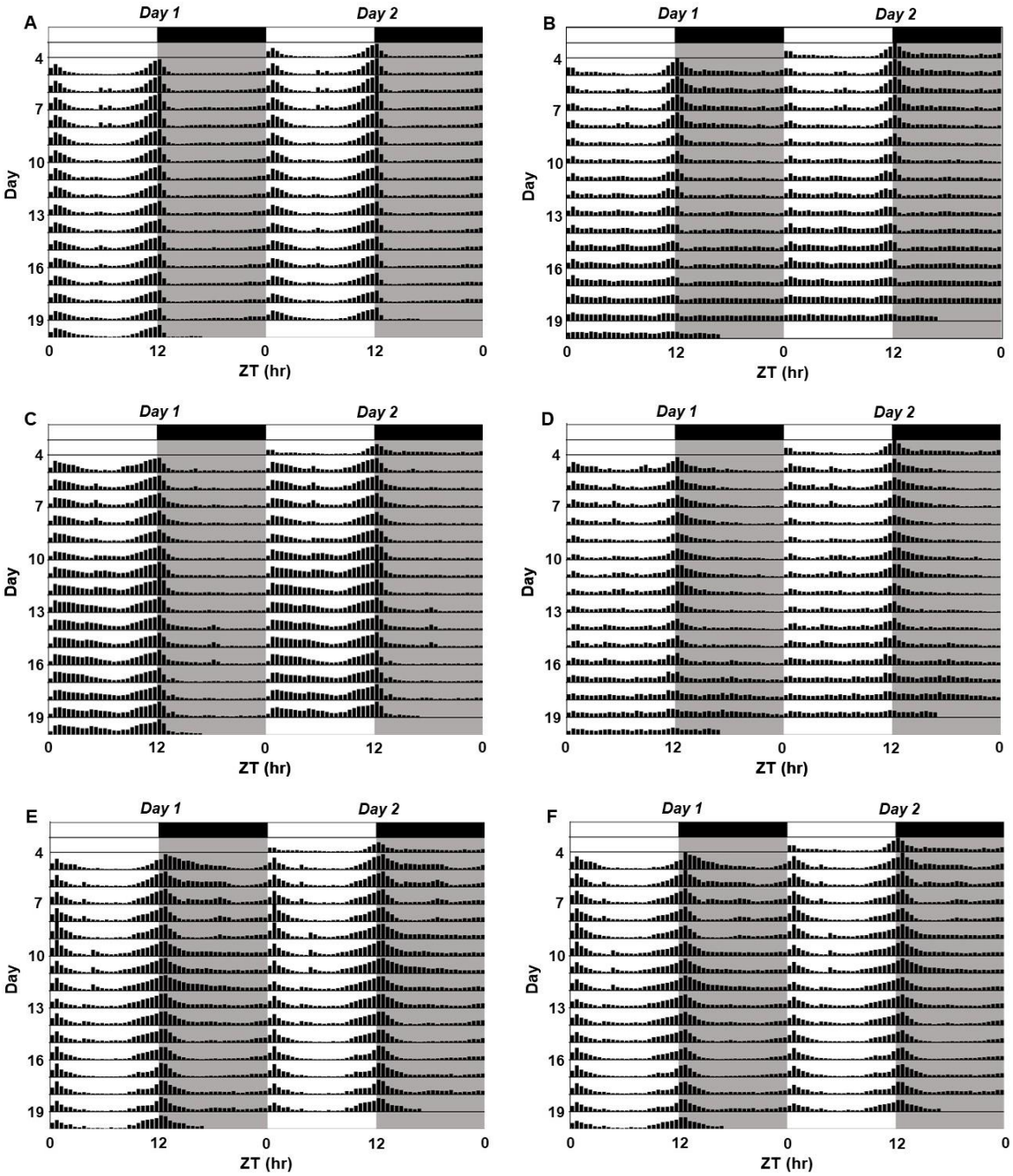

Figure 3.3. Actograms

Actogram is a graphical representation of an organism's phases of activity and rest over the course of days. Actograms are used to visualize the periodicity and rhythm in the day-to-day activity of the organisms. The figure contains the actograms for the various genotypes over the entire duration of the experiment. The x-axis represents the *Zeitgeber Time* where ZT0 is denotes D/L transition and ZT12 denotes L/D transition. Each row depicts the circadian rhythm for 2 days starting from day 4.

A) VAP^{WT} male flies. **B)** VAP^{P58S} male flies. **C)** VAP^{WT} female flies. **D)** VAP^{P58S} female flies. **E)** *CS* male flies. **F)** w^{1118} male flies.

3.3 The mutant VAP^{P58S} flies show disruption in the Sleep-Wake cycle.

Sleep in general can be defined as a state of behavioral quiescence. It is associated with a species-specific posture. In *Drosophila*, sleep is defined from a behavioral aspect as a prolonged period of inactivity. More specifically, a sleep episode (bout) is a period of inactivity/ behavioral quiescence of more than 5 minutes. Flies exhibit an increase in arousal threshold after a sleep bout (Beckwith & French, 2019). In context of the DAM system assays zero activity counts for a period of more than 5-minutes is considered as sleep. The *Drosophila* exhibit a 24hr sleep-wake cycle correlating with the circadian rhythm. Sleep primarily occurs in the middle of the day or night and the flies are more active and sleep less in anticipation of light to dark or dark to light transitions.

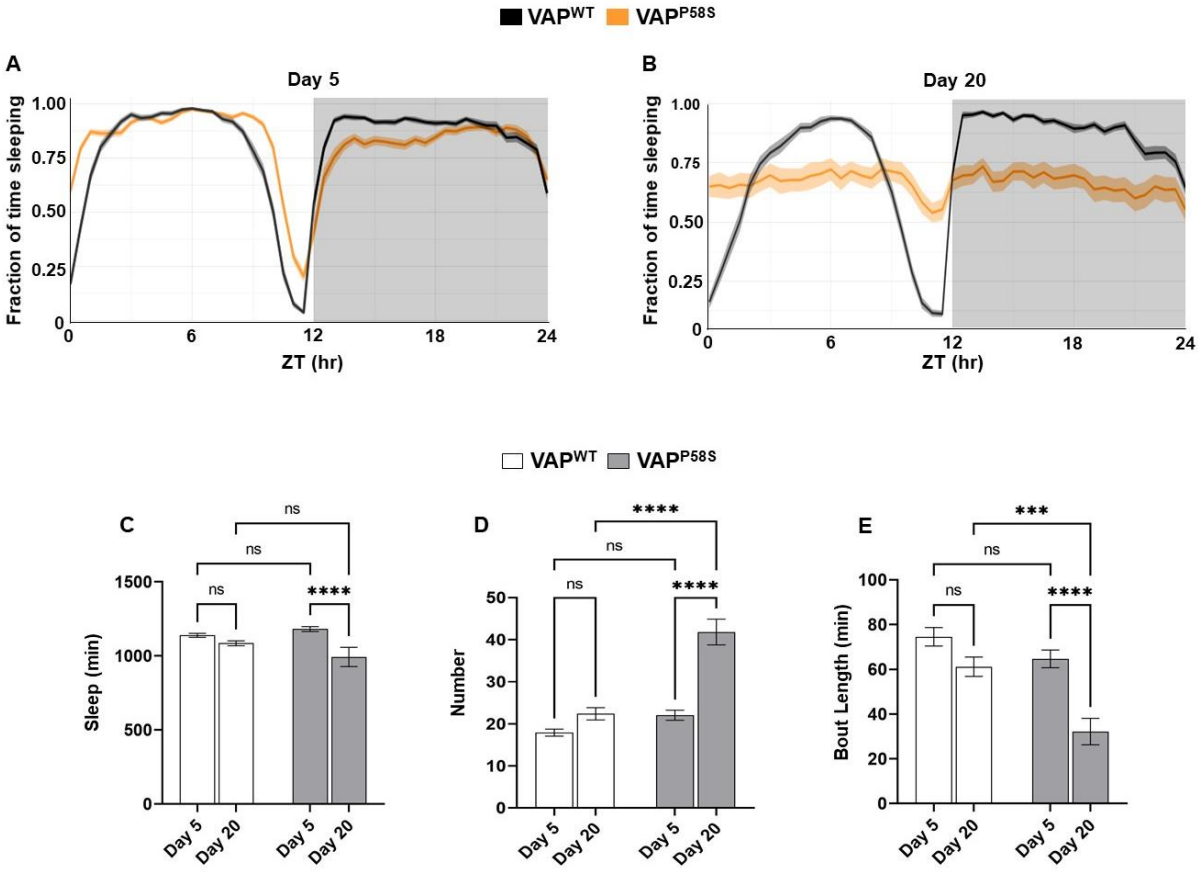

Figure 3.4. VAP^{P58S} mutant flies show disruption in sleep.
A) Sleep profile comparison for 5-days old VAP^{WT} and VAP^{P58S} flies. **B)** Sleep profile comparison for 20-days old VAP^{WT} and VAP^{P58S} flies. The x-axis for both graphs represent the *Zeitgeber Time* denoting the Light and Dark conditions. The y-axis shows the fraction of time spent sleeping per 30 min. *The sleep profiles are generated and adapted from R-based program VANESSA (Ghosh & Vasu, 2022)* **C)** The total amount of time the VAP^{P58S} flies spend sleeping decreases by day 20. **D)** The number of sleep episodes per day increase with age in VAP^{P58S} flies. **E)** Mean length of sleep episodes per day decreases with age in VAP^{P58S} flies. *The parameters are analyzed for significance using 2-way ANOVA and multiple comparisons. The significance values are determined by Tukey's t-test.* The asterisk notation depicts the *p*-values

as follows, *(ns): p>0.05, (*): p<0.05, (**): p<0.01, (***): p<0.001, (****): p<0.0001*. Exact *p*-values are mentioned in the Appendix.

The VAP^{WT} flies show the characteristic normal sleep-wake cycle which doesn't change with age. The daytime sleep shows a slight decrease going from day 5 to day 20 however, the overall sleep pattern remains the same. On the other hand, the sleep profiles for VAP^{P58S} flies show a considerable change over the duration of the assay. The VAP^{P58S} flies behave normally at younger ages and exhibit a normal sleep wake cycle. The sleep becomes more and more uniform and constant throughout the day as the flies age. The figure 3.4. A & B show the sleep profile comparisons for VAP^{WT} and VAP^{P58S} for day 5 and day 20 respectively. It is evident from the profiles that the sleep in ALS mutant flies is severely affected.

To further elucidate the effects on the sleep I compared the various sleep parameters like total sleep, number of sleep bouts and mean bout length of VAP^{WT} and VAP^{P58S} flies, for each day. The figure 3.4. C, D, E show the plots for the 3 parameters respectively. The VAP^{WT} flies show no significant changes in any of the parameters as they age. The ALS mutant flies show a decrease in the total sleep and mean bout length. In addition to this there is a considerable increase in the number of sleep bouts per day in VAP^{P58S} flies. This data very well correlates with the sleep profiles obtained from *VANESSA*. The sleep episodes of VAP^{P58S} flies becomes shorter and increase in number as they age and the flies sleep uniformly throughout the day. The flies show an increased occurrence of shorter periods of sleep/ inactivity as they age.

The female flies do show a similar pattern in their sleep behavior. However, the differences are not as significant as that of the male flies. The VAP^{WT} females sleep less in the daytime than night time as opposed to the male flies which show a similar sleep pattern in daytime as well as night time. The VAP^{P58S} female flies show a similar change in sleep profiles by the age of 20 days as that of male flies. The sleep parameters compared for female flies show no significant changes going from day 5 to day 20.

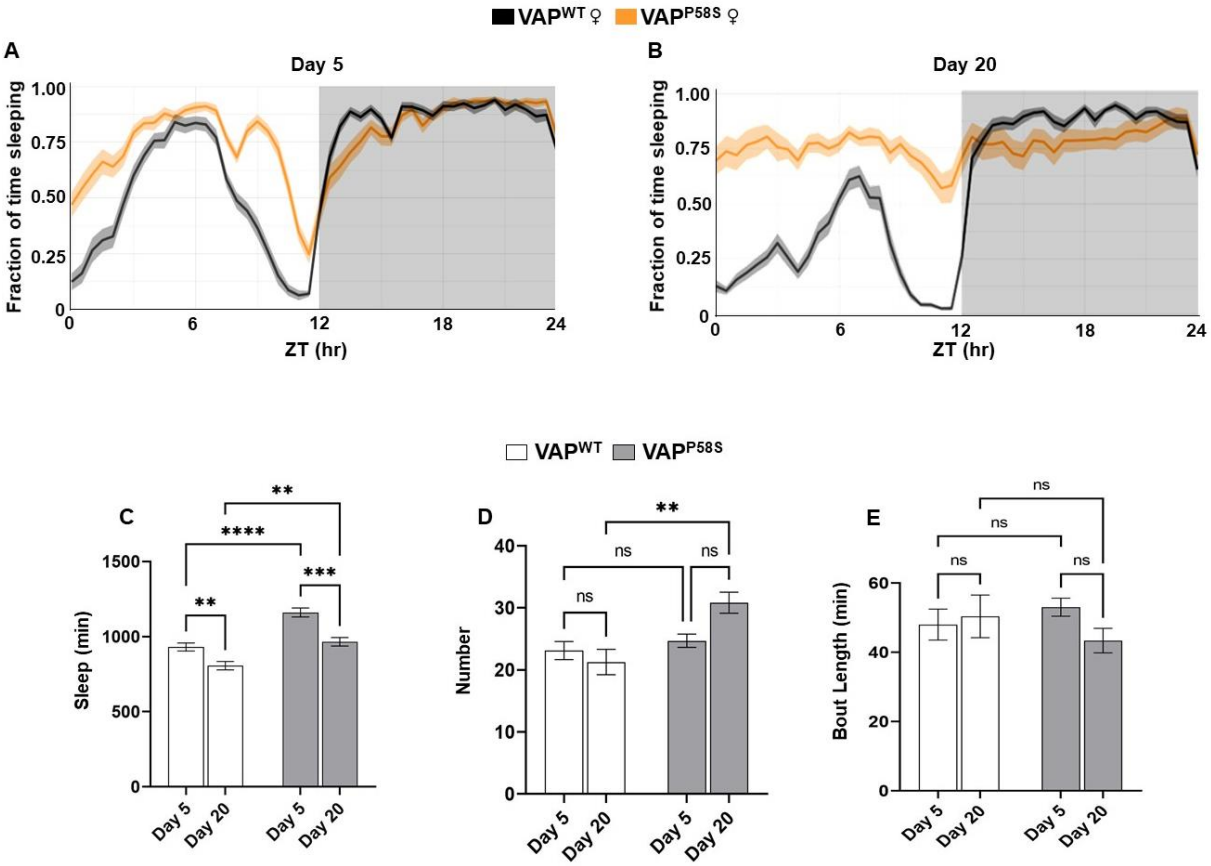

Figure 3.5. VAP^{P58S} mutant female flies show disruption in sleep.
A) Sleep profile comparison for 5-days old VAP^{WT} and VAP^{P58S} female flies. **B)** Sleep profile comparison for 20-days old VAP^{WT} and VAP^{P58S} female flies. The x-axis for both graphs represent the *Zeitgeber Time* denoting the Light and Dark conditions. The y-axis shows the fraction of time spent sleeping per 30 min. *The sleep profiles are generated and adapted from R-based program VANESSA (Ghosh & Vasu, 2022)* **C)** The total amount of time the VAP^{P58S} flies spend sleeping per day. **D)** The number of sleep episodes per day. **E)** Mean length of sleep episodes per day. *The parameters are analyzed for significance using 2-way ANOVA and multiple comparisons. The significance values are determined by Tukey's t-test.* The asterisk notation depicts the *p*-values as follows, *(ns): p>0.05, (*): p<0.05, (**): p<0.01, (***): p<0.001, (****): p<0.0001*. Exact *p*-values are mentioned in the Appendix.

3.4 The motor activity, circadian rhythm and sleep cycle is rescued by introducing a single copy of VAP^{WT}.

The results from the activity assays of VAP^{P58S} flies report deterioration in the motor function, circadian rhythm and sleep of the flies. The flies lose the periodicity in the circadian as well as sleep wake cycles with increasing age. Further, I wanted to check whether these changes in behavior patterns and loss of motor activity of VAP^{P58S} flies can be rescued by introducing a single copy of VAP^{WT}. To check for the same, I crossed the Null Rescue lines with the CRISPR lines to create fly lines exhibiting

different combinations of VAP^{P58S} and VAP^{WT}. The table 3.1 shows the detailed crosses.

Table 3.1. Schematic representation of crosses set up to obtain rescue lines.

	Parents		F1
	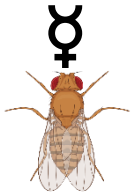 X  → 		
1	$\frac{VAP^{WT}}{VAP^{WT}}; \frac{+}{+}; \frac{+}{+}$	$\frac{\Delta VAP}{Y}; \frac{+}{+}; \frac{gVAP^{WT}}{TM3Tb}$	$\frac{VAP^{WT}}{Y}; \frac{+}{+}; \frac{gVAP^{WT}}{+}$
2	$\frac{VAP^{WT}}{VAP^{WT}}; \frac{+}{+}; \frac{+}{+}$	$\frac{\Delta VAP}{Y}; \frac{+}{+}; \frac{gVAP^{P58S}}{TM3Tb}$	$\frac{VAP^{WT}}{Y}; \frac{+}{+}; \frac{gVAP^{P58S}}{+}$
3	$\frac{VAP^{P58S}}{VAP^{P58S}}; \frac{+}{+}; \frac{+}{+}$	$\frac{\Delta VAP}{Y}; \frac{+}{+}; \frac{gVAP^{WT}}{TM3Tb}$	$\frac{VAP^{P58S}}{Y}; \frac{+}{+}; \frac{gVAP^{WT}}{+}$
4	$\frac{VAP^{P58S}}{VAP^{P58S}}; \frac{+}{+}; \frac{+}{+}$	$\frac{\Delta VAP}{Y}; \frac{+}{+}; \frac{gVAP^{P58S}}{TM3Tb}$	$\frac{VAP^{P58S}}{Y}; \frac{+}{+}; \frac{gVAP^{P58S}}{+}$

The crosses resulted in 2 types of lines, one having a double dose of either VAP^{WT} VAP^{P58S} (Here after referred to as double dosage lines) and the other type of fly line having one copy of VAP^{WT} and VAP^{P58S} each (Here after referred to as rescue lines). I carried out the DAM activity assays for these lines to check how the motor activity, circadian rhythm and sleep cycle of these flies' fairs over time.

The data from the motor activity and survival assay of these lines are shown in the figure 3.6. The motor activity of the rescue lines, VAP^{WT}; *g*VAP^{P58S} and VAP^{P58S}; *g*VAP^{WT} is considerably higher at the younger ages which decreases over time. However, the activity is comparable to that of VAP^{WT} at the age of 20 days. The rescue lines are more active and survive better as compared to the VAP^{P58S} flies. The rescue lines have a ~2 fold greater activity as compared to the VAP^{P58S} flies of the same age which is also the case for VAP^{WT} flies. It is evident from the data that a single copy of

VAP^{WT} is able to rescue the motor defects caused by VAP^{P58S} mutation. The VAP^{WT}; *g*VAP^{WT} flies show activity and survival curves comparable to that of VAP^{WT} and behave normally. The double dosage of wildtype VAP in these flies have a significant effect on the activity increasing the activity of these flies to ~100 counts per 30 minutes. The VAP^{P58S}; *g*VAP^{P58S} flies show very poor survival with a median lifespan of 17 days. More than 90% of the VAP^{P58S}; *g*VAP^{P58S} flies are dead by the end of the experiment. The flies show a steep decrease in the activity as they age. The activity on day 20 decreases to about 2.5 folds than the activity at the age of 5 days.

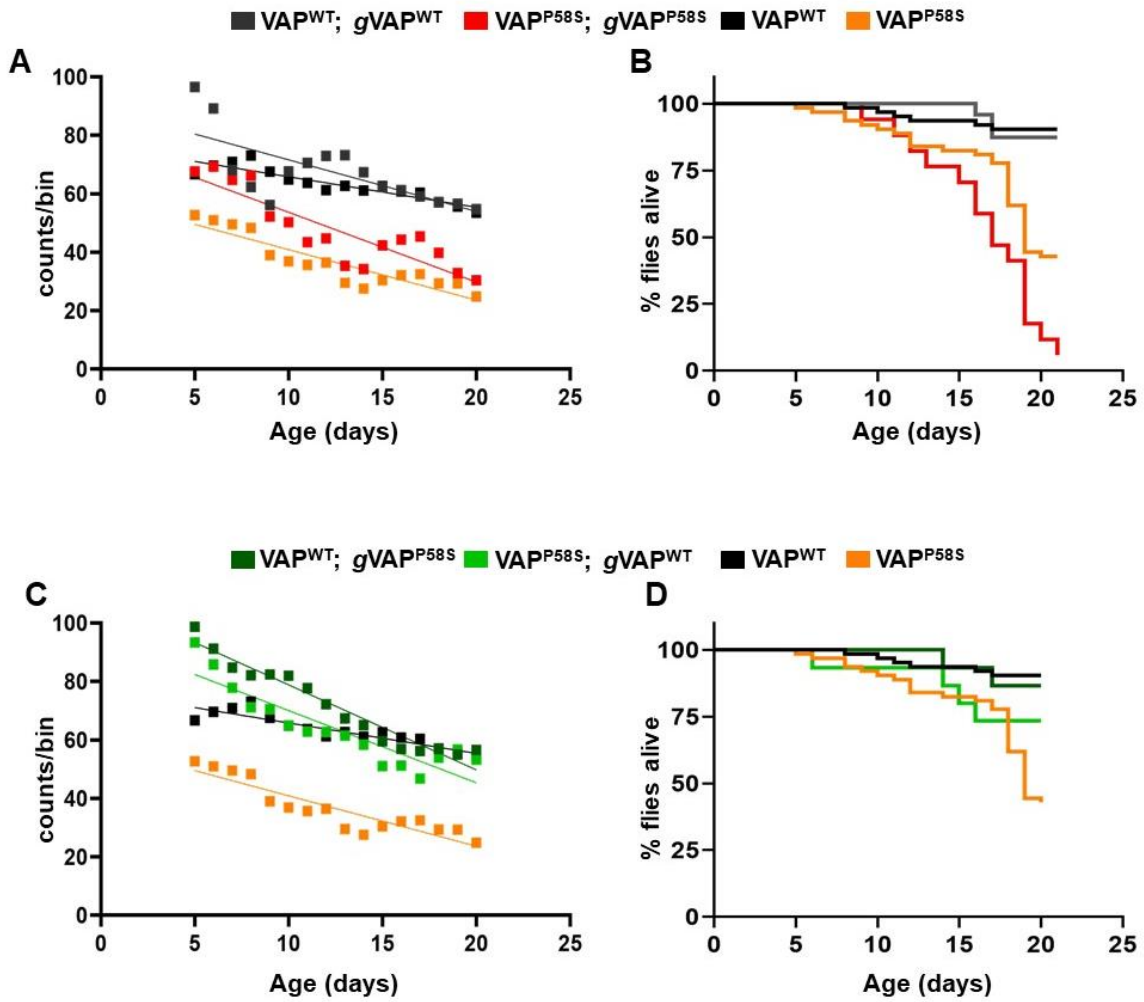

Figure 3.6. Survival and motor defects are rescued by introducing a single copy of VAP^{WT}. **A)** Motor Activity plots for VAP^{WT}; *g*VAP^{WT} (dark grey curve; n=27), VAP^{P58S}; *g*VAP^{P58S} (red curve; n=29), VAP^{WT} (control; black curve; n=32, N=2), VAP^{P58S} (orange curve; n=32; N=2) male flies. **B)** The survival curves for the same genotypes. VAP^{P58S} flies have a median lifespan of 19 days while VAP^{P58S}; *g*VAP^{P58S} have a median lifespan of 17 days. Curve comparison was done using log-rank (Mantel-Cox) test. Curves are significantly different with an overall **p-value of *p*=0.001 C)** The motor activity plots for male VAP^{WT} (black curve; n=32) and VAP^{P58S} (orange

curve; n=32) flies along with VAP^{WT}; *g*VAP^{P58S} (dark green curve; n=29) and VAP^{P58S}; *g*VAP^{WT} (light green curve; n=30) rescue lines. **D)** Survival curves for the same flies as (C). Curve comparison was done using log-rank (Mantel-Cox) test. The overall **p-value** for the four curves is ***p*=0.0905.**

The rescue lines VAP^{WT}; *g*VAP^{P58S} and VAP^{P58S}; *g*VAP^{WT} not only rescue the locomotor activity but also rescue the circadian rhythm and sleep cycle of the flies. These flies exhibit a normal circadian rhythm from age of 5 days to 20 days. They show presence of prominent activity peaks in the morning as well as evening corresponding to the dark to light and light to dark transitions respectively. The VAP^{P58S}; *g*VAP^{WT} flies show a slight disruption in the morning activity peak by the age of 20 days. However, the daily periodicity and rhythmicity of the flies remains intact.

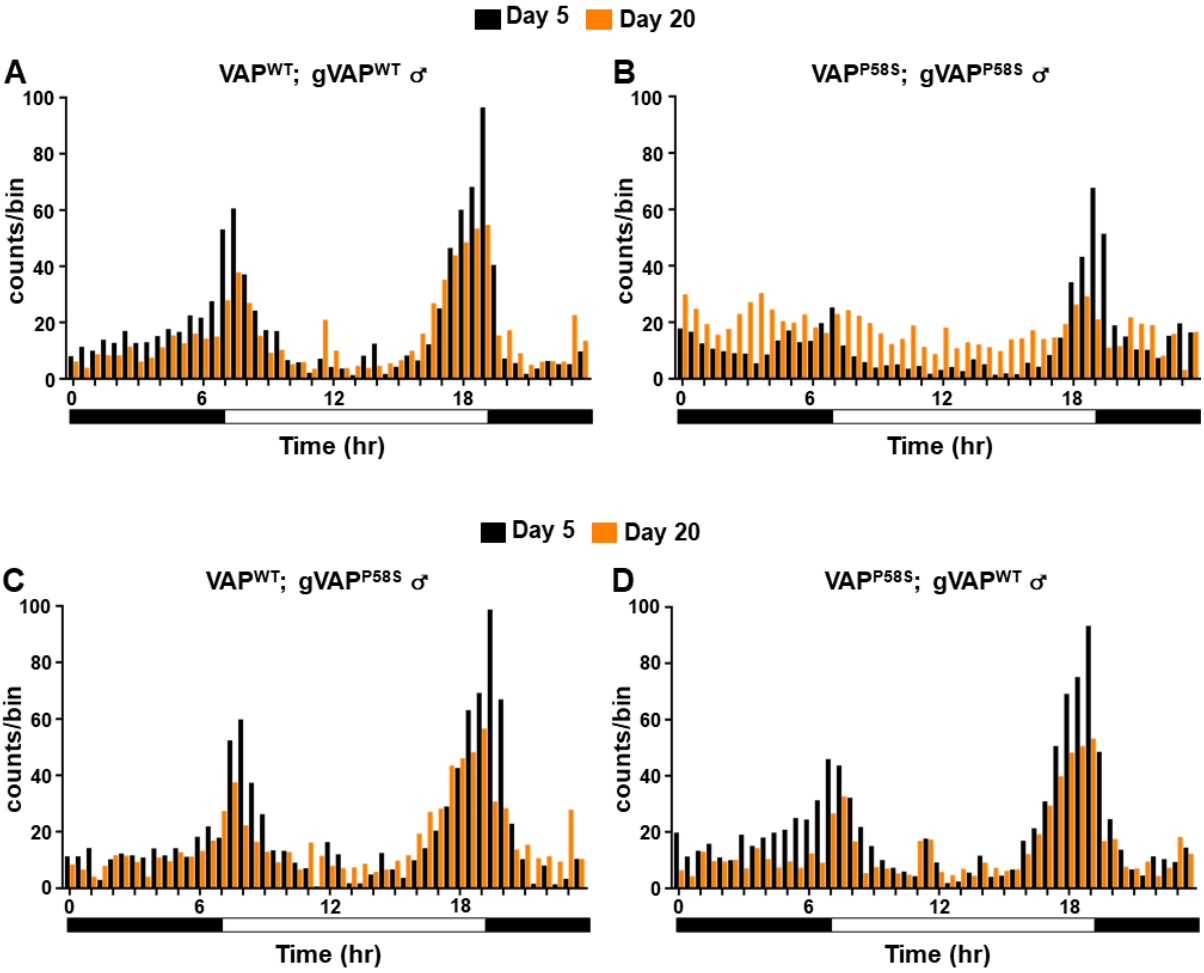

Figure 3.7. Deterioration in Circadian rhythm is rescued by introducing a single copy of VAP^{WT}.

The y-axis represents the activity counts per 30-minute bins. The x-axis represents the time of the day with 0 being 00:00:00 hrs (12:00 am). The graphs compare the circadian rhythms on day 5 and day 20 for each genotype. The bar under the x-axis shows the light-dark conditions inside the incubator. The lights are turned on at 7:00 am and are turned off at 7:00pm.

A) VAP^{WT}; *g*VAP^{WT} male flies (n=27). **B)** VAP^{P58S}; *g*VAP^{P58S} male flies (n=29). **C)** VAP^{WT}; *g*VAP^{P58S} male flies (n=29). **D)** VAP^{P58S}; *g*VAP^{WT} male flies (n=30).

The actograms for the rescue lines (Figure 3.8. C&D) very well depicts the changes in the circadian rhythm of the rescue lines overtime. The morning activity of VAP^{P58S}; *g*VAP^{WT} flies show a considerable change with the age. Though the extrachromosomal *g*VAP^{WT} introduced on the 3rd chromosome is able to rescue the daily rhythm the effect of chromosomal VAP^{P58S} may be the cause of the deterioration in the morning activity.

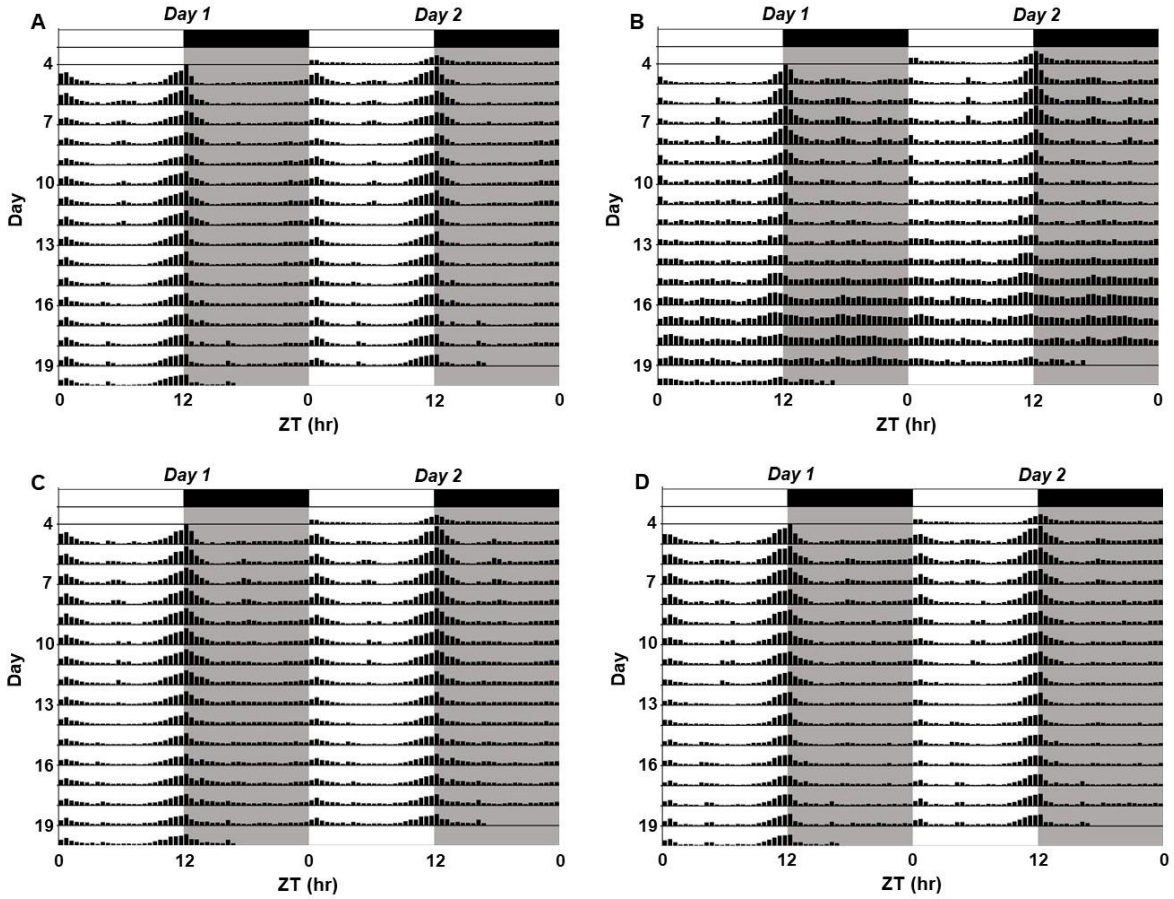

Figure 3.8. Actograms for rescue and double dosage lines
Actogram is a graphical representation of an organism's phases of activity and rest over the course of days. Actograms are used to visualize the periodicity and rhythm in the day-to-day activity of the organisms. The figure contains the actograms for the various genotypes over the entire duration of the experiment. The x-axis represents the *Zeitgeber Time* where ZT0 is denotes D/L transition and ZT12 denotes L/D transition. Each row depicts the circadian rhythm for 2 days starting from day 4.
A) *VAP^{WT}; gVAP^{WT}* male flies. **B)** VAP^{P58S}; *g*VAP^{P58S} male flies. **C)** VAP^{WT}; *g*VAP^{P58S} male flies. **D)** VAP^{P58S}; *g*VAP^{WT} male flies.

The wildtype double dosage line VAP^{WT}; *g*VAP^{WT} exhibits normal circadian rhythms comparable to that of VAP^{WT}. The VAP^{P58S}; *g*VAP^{P58S} flies lose the circadian rhythm completely by the age of 20 days. As compared to the flies carrying a single copy of VAP^{P58S} the double dosage mutant flies show drastic changes in the daily activity patterns. The periodicity in the activity patterns of VAP^{P58S}; *g*VAP^{P58S} flies is lost by the age of ~14 days and the flies become arrhythmic. Even at the age of 5 days the morning activity peak is not prominent in these flies and the morning activity is very low as compared to that of the evening activity. The data suggests that there may be a dosage dependency for how the VAP^{P58S} mutation affects the circadian behavior of the flies.

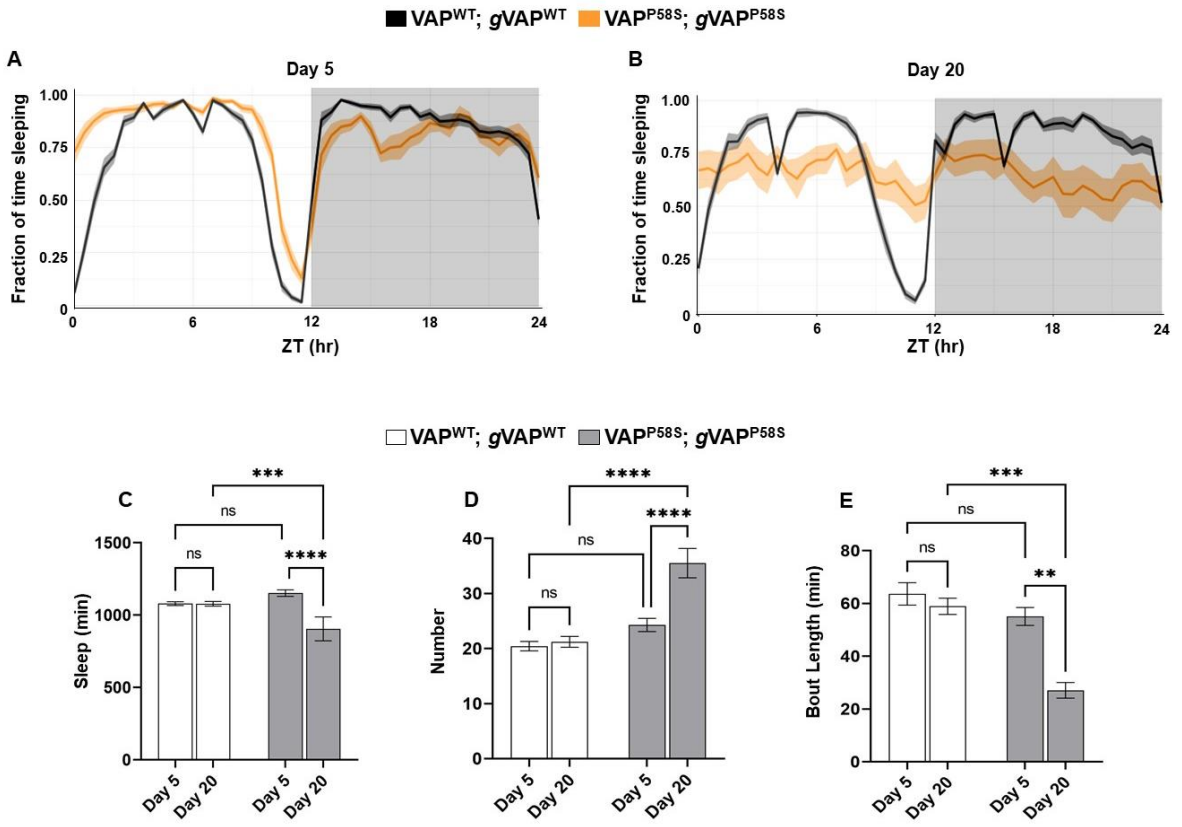

Figure 3.9. VAP^{P58S}; *g*VAP^{P58S} show disruption in sleep
A) Sleep profile comparison for 5-days old VAP^{WT}; *g*VAP^{WT} and VAP^{P58S}; *g*VAP^{P58S} flies. **B)** Sleep profile comparison for 20-days old VAP^{WT}; *g*VAP^{WT} and VAP^{P58S}; *g*VAP^{P58S} flies. The x-axis for both graphs represent the *Zeitgeber Time* denoting the Light and Dark conditions. The y-axis shows the fraction of time spent sleeping per 30 min. *The sleep profiles are generated and adapted from R-based program VANESSA (Ghosh & Vasu, 2022)* **C)** The total amount of time the VAP^{P58S}; *g*VAP^{P58S} flies spend sleeping decreases by day 20. **D)** The number of sleep episodes per day increase with age in VAP^{P58S}; *g*VAP^{P58S} flies. **E)** Mean length of sleep episodes per day decreases with age in VAP^{P58S}; *g*VAP^{P58S} flies. *The parameters are analyzed for significance using 2-way ANOVA and multiple comparisons. The significance values are determined by Tukey's t-test.* The asterisk notation depicts the *p*-values as follows, *(ns): p>0.05,*

(*): p<0.05, (**): p<0.01, (***): p<0.001, (****): p<0.0001. Exact *p*-values are mentioned in the Appendix.

I further analyzed the sleep patterns for the rescue and double dosage lines. The sleep patterns of the rescue lines and the VAP^{WT}; *g*VAP^{WT} are comparable to that of VAP^{WT} flies. They exhibit a normal sleep profile throughout the span of the assay and doesn't show any significant changes in the sleep parameters. The VAP^{P58S}; *g*VAP^{P58S} flies however show considerable changes in the sleep patterns and the sleep parameters like total sleep, number of bouts and mean bout lengths. Similar to that of the flies carrying a single copy of VAP^{P58S} the double dosage mutant flies also show reduction in the total sleep per day as they age. The mean sleep bout lengths are decreased by almost 50% by the age of 20 days. The number of sleep episodes each day increase with the increase in the age.

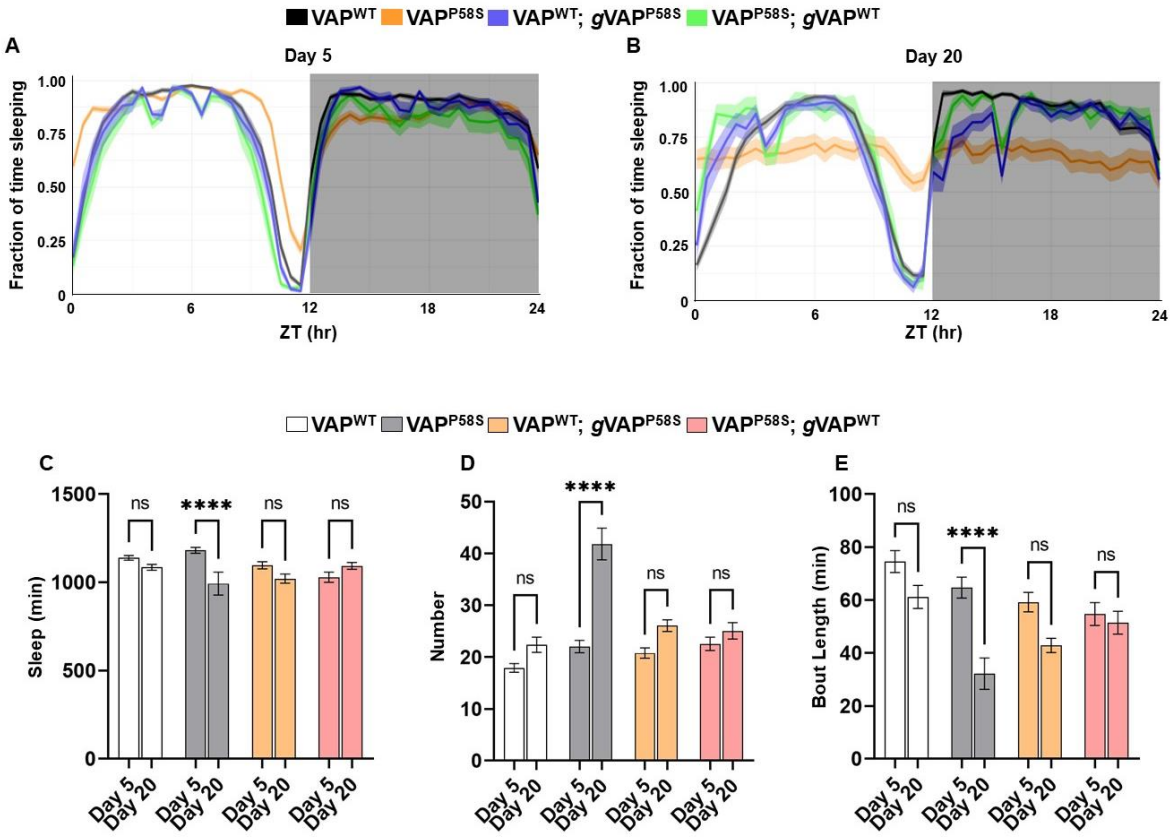

Figure 3.10. Disruption in Sleep cycles is rescued by introducing a single copy of VAP^{WT}. **A)** Sleep profile comparison for 5-days old VAP^{WT}; *g*VAP^{P58S} and VAP^{P58S}; *g*VAP^{WT} rescue line flies along with VAP^{WT} and VAP^{P58S} mutant flies. **B)** Sleep profile comparison for 20-days old VAP^{WT}; *g*VAP^{P58S} and VAP^{P58S}; *g*VAP^{WT} rescue line flies along with VAP^{WT} and VAP^{P58S} mutant flies. The x-axis for both graphs represent the *Zeitgeber Time* denoting the Light and Dark conditions. The y-axis shows the fraction of time spent sleeping per 30 min. *The sleep profiles are generated and adapted from R-based program VANESSA (Ghosh & Vasu, 2022)* **C)** The

total amount of time spent sleeping per day. **D)** The number of sleep episodes per day. **E)** Mean length of sleep episodes per day. *The parameters are analyzed for significance using 2-way ANOVA and multiple comparisons. The significance values are determined by Tukey's t-test.* The asterisk notation depicts the *p*-values as follows, *(ns): p>0.05, (*): p<0.05, (**): p<0.01, (***): p<0.001, (****): p<0.0001*. Exact *p*-values are mentioned in the Appendix.

The Rescue lines exhibit normal sleep behavior and sleep parameters. The parameter values are comparable to that of VAP^{WT} flies and are shown in the figure 3.10. The rescue lines display a normal sleep-wake cycle from age of 5 days to 20 days. The sleep profiles for both VAP^{WT}; *g*VAP^{P58S} & VAP^{P58S}; *g*VAP^{WT} flies are similar to that of VAP^{WT}. The rescue lines show no significant changes in the total sleep, number of sleep episodes and mean sleep bout lengths per day. The defects in the sleep exhibited by the VAP^{P58S} flies are rescued by adding a single copy of VAP^{WT}.

Chapter 4: Discussion

A point mutation (P58S) in the VAP-33A gene causes the animal to show ALS like symptoms in flies. Adult flies carrying the VAP^{P58S} mutation exhibit progressive motor defects. These flies also have a shorter (~30%) lifespan as compared to that of wildtype flies. In addition, the mutant flies also showed behavioral changes, including age-dependent deterioration in the circadian rhythm and perturbation in sleep-wake cycles. Specifically, the flies lose the periodicity in their circadian activity and become arrhythmic with increasing age. The sleep patterns are also hindered with the mutant flies sleeping less as they age. Unlike in wild-type animals, sleep is uniformly distributed throughout the day with increased number of shorter sleep bouts. Thus, the generation and characterization of this mutant line generates a *Drosophila* ALS model which will allow us to study mechanisms that underly the initiation and progression of human disease.

Interestingly, these effects on motor functions and behavior of the flies can be rescued by introducing a single copy of VAP^{WT} along with the VAP^{P58S} mutation. The 'rescued' flies exhibit normal circadian and sleep behavior. The motor functions, circadian rhythms, sleep and lifespan are at par with wild-type animals. The above statement is true for both males and females, though there are subtle differences between the two.

The female VAP^{P58S} flies, similar to that of the male ALS mutant flies exhibit progressive motor defects and behavioral changes. The female flies generally display a different pattern in daily activity as compared to the male flies. The female flies sleep less in the daytime and are more active in this time period. The female ALS mutant flies show a trend similar to that of male VAP^{P58S} flies in the deterioration of circadian rhythms and perturbation in daily sleep profiles. The flies become arrhythmic as they age. The sleep in female flies become fragmented with shorter sleep bouts.

It is evident from the results obtained from this study that the mutation in the VAP gene in *Drosophila* not only affects the motor function of the subject but also alters the behavior. The previous studies from our lab have shown that the ALS causes changes in the NMJ morphology (Tendulkar, 2020). Also, as mentioned before, the

VAP^{P58S} flies show presence of VAP positive brain aggregates. Thus, VAP plays a significant role in neuronal, especially motor neuronal functions.

The behavioral patterns in *Drosophila* like the circadian rhythm and Sleep-Wake cycles are controlled by the clock neurons in the brain. The core clock network consists of a set of ~150 neurons clustered into discrete groups in the brain. (Dubowy & Sehgal, 2017). A recent study (Faragó et al., 2019) in Huntington Disease (HD) model flies have shown that the HD flies have fragmented sleep with prolonged sleep latency. The clock gene expression patterns in these HD model flies showed disordered regulation of core feedback loop genes like *per* and *tim*. Other neurodegenerative diseases like Alzheimer's' and Parkinson's disease also show defects in circadian and sleep rhythms (Buhl et al. 2019).

The changes in the behavioral patterns observed in the VAP^{P58S} mutant flies can be explained on the similar lines. The mutation in VAP causes misfolding of MSP domain which is then unable to be cleaved and secreted to carry out downstream processes. The mutation causes aggregation of VAP in cells and disrupts various cellular process leading to motor neurodegeneration. We hypothesize that VAP may be part of a gene regulatory network that includes the circadian clock genes like *per* and *tim.* The mutation in VAP causes disruption in this network and regulation of clock genes like observed in HD.

Another possibility is that the neurons regulating the clock are also deteriorating, in parallel with their motor-neuron counterparts. If this is true, we could use clock-neuron specific Gal4 lines to rescue only in the clock neurons, by expressing VAP^{WT} specifically in these neurons. Any delay in degeneration of clock neurons would rescue only the circadian/sleep phenotypes and not the age dependent motor deterioration. Another interesting experiment would be to repeat the same set of experiments in complete darkness rather than a 12h:12h L/D cycle. This will also help to gain an insight into the functioning of circadian clock regulators in the VAP^{P58S} mutant flies.

Many physicians caring for ALS patients have reported changes in the patients' behavior and cognitive functions. We were able to show through this study that the *Drosophila* model for ALS also exhibits behavioral defects, which can be rescued by

a single copy of wildtype gene. The study implies that VAP may have a role in regulation of the circadian clock in *Drosophila.*

We would like to further investigate how mutation in VAP causes behavioral changes in *Drosophila.* Analysing the expression patterns of clock genes in a VAP^{P58S} background to check whether regulation of the core clock genes is disrupted in the ALS will help in better understanding the role of VAP^{P58S} in controlling *Drosophila* behavior. We would like to investigate whether VAP directly interacts with any of the clock network genes regulating their function. Expressing or knocking down VAP specifically in the clock neurons and monitoring the fly activities will further clarify the role of VAP in *Drosophila* behavior. We further plan to use the diverse genetic toolkit available in *Drosophila* to probe for molecular relationships between neurodegenerative disease and behavior.

Chapter 5: Appendix

5.1 Table of *p*-values for Survival Curves

Results for Log-rank (Mantel-Cox) Test	
Figure 3.1. (B) Survival Curves for Male ALS mutant Flies	
Chi Square	12.96
Df	3
p-value	0.0047
p-value summary	**
Are the curves significantly different?	Yes
Figure 3.1. (D) Survival Curves for Female ALS mutant Flies	
Chi Square	23.20
Df	3
p-value	0.00037
p-value summary	****
Are the curves significantly different?	Yes
Figure 3.6. (B) Survival Curves for Double Dosage Lines	
Chi Square	20.97
Df	3
p-value	0.0001
p-value summary	***
Are the curves significantly different?	Yes
Figure 3.6. (D) Survival Curves for Rescue Lines	
Chi Square	6.480
Df	3
p-value	0.0905
p-value summary	ns
Are the curves significantly different?	No

5.2 Results for 2-way ANOVA

ANOVA table for Sleep Parameter Graphs					
Figure 3.4. (C) Total Sleep Comparison for Male ALS mutant Flies					
	Sum of Squares (Type III)	**Df**	**Mean Square**	**F-value**	***p*-value**
Interaction	219285	1	219285	7.449	0.0069
Row (Age of Flies)	703668	1	703668	23.90	0.000002
Column (Genotype)	29561	1	29561	1.004	0.3174
Residual	6181717	210	29437		
Figure 3.4. (D) Number of Sleep Bout Comparison for Male ALS mutant Flies					
	Sum of Squares (Type III)	**Df**	**Mean Square**	**F-value**	***p*-value**
Interaction	2815	1	2815	25.60	<0.000001
Row (Age of Flies)	7087	1	7087	64.46	<0.000001
Column (Genotype)	6668	1	6668	60.65	<0.000001
Residual	23087	210	109.9		
Figure 3.4. (E) Mean Sleep Bout Length Comparison for Male ALS mutant Flies					
	Sum of Squares (Type III)	**Df**	**Mean Square**	**F-value**	***p*-value**
Interaction	4412	1	4412	4.173	0.042312
Row (Age of Flies)	25330	1	25330	23.96	0.000002
Column (Genotype)	18154	1	18154	17.17	0.000049
Residual	221987	210	1057		

Figure 3.5. (C) Total Sleep Comparison for Female ALS mutant Flies					
	Sum of Squares (Type III)	**Df**	**Mean Square**	**F-value**	***p*-value**
Interaction	31806	1	31806	1.356	0.246883
Row (Age of Flies)	660721	1	660721	28.16	<0.000001
Column (Genotype)	977435	1	977435	41.66	<0.000001
Residual	2510439	107	23462		
Figure 3.5. (D) Number of Sleep Bout Comparison for Female ALS mutant Flies					
	Sum of Squares (Type III)	**Df**	**Mean Square**	**F-value**	***p*-value**
Interaction	412.0	1	412.0	5.764	0.018083
Row (Age of Flies)	117.7	1	117.7	1.646	0.202215
Column (Genotype)	801.3	1	801.3	11.21	0.001123
Residual	7647	107	71.47		
Figure 3.5. (E) Mean Sleep Bout Length Comparison for Female ALS mutant Flies					
	Sum of Squares (Type III)	**Df**	**Mean Square**	**F-value**	***p*-value**
Interaction	935.1	1	935.1	1.593	0.209700
Row (Age of Flies)	342.1	1	342.1	0.5827	0.446954
Column (Genotype)	25.14	1	25.14	0.04282	0.836452
Residual	62828	107	587.2		

Figure 3.9. (C) Total Sleep Comparison for Double Dosage Lines					
	Sum of Squares (Type III)	**Df**	**Mean Square**	**F-value**	***p*-value**
Interaction	230204	1	230204	21.05	0.000019
Row (Age of Flies)	235143	1	235143	21.50	0.000016
Column (Genotype)	39239	1	39239	3.588	0.062255
Residual	776368	71	10935		
Figure 3.9. (D) Number of Sleep Bout Comparison for Double Dosage Lines					
	Sum of Squares (Type III)	**Df**	**Mean Square**	**F-value**	***p*-value**
Interaction	414.6	1	414.6	16.42	0.000128
Row (Age of Flies)	548.3	1	548.3	21.72	0.000014
Column (Genotype)	1252	1	1252	49.59	<0.000001
Residual	1793	71	25.25		
Figure 3.9. (E) Mean Sleep Bout Length Comparison for Double Dosage Lines					
	Sum of Squares (Type III)	**Df**	**Mean Square**	**F-value**	***p*-value**
Interaction	2065	1	2065	6.985	0.010108
Row (Age of Flies)	4085	1	4085	13.81	0.000399
Column (Genotype)	6211	1	6211	21.00	0.000019
Residual	20995	71	295.7		

Figure 3.10. (C) Total Sleep Comparison for Rescue Lines					
	Sum of Squares (Type III)	**Df**	**Mean Square**	**F-value**	***p*-value**
Interaction	388106	3	129369	5.115	0.001867
Row (Age of Flies)	170928	1	170928	6.758	0.009860
Column (Genotype)	106323	3	35441	1.401	0.242813
Residual	6626189	262	25291		
Figure 3.10. (D) Number of Sleep Bout Comparison for Rescue Lines					
	Sum of Squares (Type III)	**Df**	**Mean Square**	**F-value**	***p*-value**
Interaction	3305	3	1102	11.93	<0.000001
Row (Age of Flies)	2738	1	2738	29.65	<0.000001
Column (Genotype)	6731	3	2244	24.29	<0.000001
Residual	24198	262	92.36		
Figure 3.10. (E) Mean Sleep Bout Length Comparison for Rescue Lines					
	Sum of Squares (Type III)	**Df**	**Mean Square**	**F-value**	***p*-value**
Interaction	6245	3	2082	2.343	0.073545
Row (Age of Flies)	11444	1	11444	12.88	0.000396
Column (Genotype)	21101	3	7034	7.916	0.000045
Residual	232790	262	888.5		

Tukey's Test Results for Sleep Parameter Graphs		
Figure 3.4. (C) Total Sleep Comparison for Male ALS mutant Flies		
Compared Groups	***p*-value**	**Summary of *p*-value**
Day 5:VAP^{WT} vs. Day 5:VAP^{P58S}	0.498378	ns
Day 5:VAP^{WT} vs. Day 20:VAP^{WT}	0.316665	ns
Day 5:VAP^{P58S} vs. Day 20:VAP^{P58S}	0.000011	****
Day 20:VAP^{WT} vs. Day 20:VAP^{P58S}	0.086802	ns
Figure 3.4. (D) Number of Sleep Bout Comparison for Male ALS mutant Flies		
Compared Groups	***p*-value**	**Summary of *p*-value**
Day 5:VAP^{WT} vs. Day 5:VAP^{P58S}	0.121984	ns
Day 5:VAP^{WT} vs. Day 20:VAP^{WT}	0.087695	ns
Day 5:VAP^{P58S} vs. Day 20:VAP^{P58S}	<0.000001	****
Day 20:VAP^{WT} vs. Day 20:VAP^{P58S}	<0.000001	****
Figure 3.4. (E) Mean Sleep Bout Length Comparison for Male ALS mutant Flies		
Compared Groups	***p*-value**	**Summary of *p*-value**
Day 5:VAP^{WT} vs. Day 5:VAP^{P58S}	0.322197	ns
Day 5:VAP^{WT} vs. Day 20:VAP^{WT}	0.108578	ns
Day 5:VAP^{P58S} vs. Day 20:VAP^{P58S}	0.000078	****
Day 20:VAP^{WT} vs. Day 20:VAP^{P58S}	0.000678	***

Figure 3.5. (C) Total Sleep Comparison for Female ALS mutant Flies		
Compared Groups	***p*-value**	**Summary of *p*-value**
Day 5:VAP^{WT} vs. Day 5:VAP^{P58S}	<0.000001	****
Day 5:VAP^{WT} vs. Day 20:VAP^{WT}	0.009497	**
Day 5:VAP^{P58S} vs. Day 20:VAP^{P58S}	0.000275	***
Day 20:VAP^{WT} vs. Day 20:VAP^{P58S}	0.004749	**

Figure 3.5. (D) Number of Sleep Bout Comparison for Female ALS mutant Flies		
Compared Groups	***p*-value**	**Summary of *p*-value**
Day 5:VAP^{WT} vs. Day 5:VAP^{P58S}	0.878513	ns
Day 5:VAP^{WT} vs. Day 20:VAP^{WT}	0.822941	ns
Day 5:VAP^{P58S} vs. Day 20:VAP^{P58S}	0.080588	ns
Day 20:VAP^{WT} vs. Day 20:VAP^{P58S}	0.001767	**
Figure 3.5. (E) Mean Sleep Bout Length Comparison for Female ALS mutant Flies		
Compared Groups	***p*-value**	**Summary of *p*-value**
Day 5:VAP^{WT} vs. Day 5:VAP^{P58S}	0.840196	ns
Day 5:VAP^{WT} vs. Day 20:VAP^{WT}	0.980376	ns
Day 5:VAP^{P58S} vs. Day 20:VAP^{P58S}	0.547945	ns
Day 20:VAP^{WT} vs. Day 20:VAP^{P58S}	0.777095	ns

Figure 3.9. (C) Total Sleep Comparison for Double Dosage Lines		
Compared Groups	***p*-value**	**Summary of *p*-value**
Day 5:VAP^{WT};*g*VAP^{WT} vs. Day 5:VAP^{P58S};*g*VAP^{P58S}	0.114806	ns
Day 5:VAP^{WT};*g*VAP^{WT} vs. Day 20:VAP^{WT};*g*VAP^{WT}	0.999970	ns
Day 5:VAP^{P58S};*g*VAP^{P58S} vs. Day 20:VAP^{P58S};*g*VAP^{P58S}	0.000003	****
Day 20:VAP^{WT};*g*VAPWT vs. Day 20:VAP^{P58S};*g*VAP^{P58S}	0.000792	***
Figure 3.9. (D) Number of Sleep Bout Comparison for Double Dosage Lines		
Compared Groups	***p*-value**	**Summary of *p*-value**
Day 5:VAP^{WT};*g*VAP^{WT} vs. Day 5:VAP^{P58S};*g*VAP^{P58S}	0.065462	ns
Day 5:VAP^{WT};*g*VAP^{WT} vs. Day 20:VAP^{WT};*g*VAP^{WT}	0.948245	ns
Day 5:VAP^{P58S};*g*VAP^{P58S} vs. Day 20:VAP^{P58S};*g*VAP^{P58S}	0.000009	****
Day 20:VAP^{WT};*g*VAPWT vs. Day 20:VAP^{P58S};*g*VAP^{P58S}	<0.000001	****

Figure 3.9. (E) Mean Sleep Bout Length Comparison for Double Dosage Lines		
Compared Groups	***p*-value**	**Summary of *p*-value**
Day 5:VAP^{WT};*g*VAP^{WT} vs. Day 5:VAP^{P58S};*g*VAP^{P58S}	0.365916	ns
Day 5:VAP^{WT};*g*VAP^{WT} vs. Day 20:VAP^{WT};*g*VAP^{WT}	0.773054	ns
Day 5:VAP^{P58S};*g*VAP^{P58S} vs. Day 20:VAP^{P58S};*g*VAP^{P58S}	0.001489	**
Day 20:VAP^{WT};*g*VAPWT vs. Day 20:VAP^{P58S};*g*VAP^{P58S}	0.000157	***

Figure 3.10. (C) Total Sleep Comparison for Rescue Lines		
Compared Groups	***p*-value**	**Summary of *p*-value**
Day 5:VAP^{WT} vs. Day 20:VAP^{WT}	0.583788	ns
Day 5:VAP^{P58S} vs. Day 20:VAP^{P58S}	0.000007	****
Day 5:VAP^{WT};*g*VAP^{P58S} vs. Day 20:VAP^{WT};*g*VAP^{P58S}	0.909646	ns
Day 5:VAP^{P58S};*g*VAP^{WT} vs. Day 20:VAP^{P58S};*g*VAP^{WT}	0.970483	ns
Figure 3.10. (D) Number of Sleep Bout Comparison for Rescue Lines		
Compared Groups	***p*-value**	**Summary of *p*-value**
Day 5:VAP^{WT} vs. Day 20:VAP^{WT}	0.255994	ns
Day 5:VAP^{P58S} vs. Day 20:VAP^{P58S}	<0.000001	****
Day 5:VAP^{WT};*g*VAP^{P58S} vs. Day 20:VAP^{WT};*g*VAP^{P58S}	0.985797	ns
Day 5:VAP^{P58S};*g*VAP^{WT} vs. Day 20:VAP^{P58S};*g*VAP^{WT}	>0.999999	ns
Figure 3.10. (E) Mean Sleep Bout Length Comparison for Rescue Lines		
Compared Groups	***p*-value**	**Summary of *p*-value**
Day 5:VAP^{WT} vs. Day 20:VAP^{WT}	0.210734	ns
Day 5:VAP^{P58S} vs. Day 20:VAP^{P58S}	0.000054	****
Day 5:VAP^{WT};*g*VAP^{P58S} vs. Day 20:VAP^{WT};*g*VAP^{P58S}	0.822637	ns
Day 5:VAP^{P58S};*g*VAP^{WT} vs. Day 20:VAP^{P58S};*g*VAP^{WT}	0.999992	ns

References:

Armon C. (2009). Smoking may be considered an established risk factor for sporadic ALS. Neurology, 73(20), 1693–1698. ttps://doi.org/10.1212/WNL.0b013e3181c1df48

Beckwith, E. J., & French, A. S. (2019). Sleep in Drosophila and Its Context. Frontiers in physiology, 10, 1167. https://doi.org/10.3389/fphys.2019.01167

bioRxiv doi: https://doi.org/10.1101/2021.04.07.438776

Buhl, E., Higham, J. P., & Hodge, J. (2019). Alzheimer's disease-associated tau alters Drosophila circadian activity, sleep and clock neuron electrophysiology. Neurobiology of disease, 130, 104507. https://doi.org/10.1016/j.nbd.2019.104507

Deivasigamani, S., Verma, H. K., Ueda, R., Ratnaparkhi, A., & Ratnaparkhi, G. S. (2014). A genetic screen identifies Tor as an interactor of VAPB in a Drosophila model of amyotrophic lateral sclerosis. Biology open, 3(11), 1127–1138. https://doi.org/10.1242/bio.201410066

Dubowy, C., & Sehgal, A. (2017). Circadian Rhythms and Sleep in Drosophila melanogaster. Genetics, 205(4), 1373–1397. https://doi.org/10.1534/genetics.115.185157

Faragó, A., Zsindely, N., & Bodai, L. (2019). Mutant huntingtin disturbs circadian clock gene expression and sleep patterns in Drosophila. Scientific reports, 9(1), 7174. https://doi.org/10.1038/s41598-019-43612-w

Goetz C. G. (2000). Amyotrophic lateral sclerosis: early contributions of Jean-Martin Charcot. Muscle & nerve, 23(3), 336–343. https://doi.org/10.1002/(sici)1097-4598(200003)23:3<336::aid-mus4>3.0.co;2-l

https://www.nigms.nih.gov/education/fact-sheets/Pages/circadian-rhythms.aspx

Jaiswal M. K. (2019). Riluzole and edaravone: A tale of two amyotrophic lateral sclerosis drugs. Medicinal research reviews, 39(2), 733–748. https://doi.org/10.1002/med.21528

James, C., & Kehlenbach, R. H. (2021). The Interactome of the VAP Family of Proteins: An Overview. *Cells*, *10*(7), 1780. https://doi.org/10.3390/cells10071780

Kim, S., Leal, S. S., Ben Halevy, D., Gomes, C. M., & Lev, S. (2010). Structural requirements for VAP-B oligomerization and their implication in amyotrophic lateral sclerosis-associated VAP-B(P56S) neurotoxicity. The Journal of biological chemistry, 285(18), 13839–13849. https://doi.org/10.1074/jbc.M109.097345

Kumar, D. R., Aslinia, F., Yale, S. H., & Mazza, J. J. (2011). Jean-Martin Charcot: the father of neurology. Clinical medicine & research, 9(1), 46–49. https://doi.org/10.3121/cmr.2009.883

Kume, K., Kume, S., Park, S. K., Hirsh, J., & Jackson, F. R. (2005). Dopamine is a regulator of arousal in the fruit fly. The Journal of neuroscience : the official journal of the Society for Neuroscience, 25(32), 7377–7384. https://doi.org/10.1523/JNEUROSCI.2048-05.2005

Marques, V. D., Barreira, A. A., Davis, M. B., Abou-Sleiman, P. M., Silva, W. A., Jr, Zago, M. A., Sobreira, C., Fazan, V., & Marques, W., Jr (2006). Expanding the phenotypes of the Pro56Ser VAPB mutation: proximal SMA with dysautonomia. Muscle & nerve, 34(6), 731–739. https://doi.org/10.1002/mus.20657

Martin, S., Al Khleifat, A., & Al-Chalabi, A. (2017). What causes amyotrophic lateral sclerosis?. F1000Research, 6, 371. https://doi.org/10.12688/f1000research.10476.1

Masrori, P., & Van Damme, P. (2020). Amyotrophic lateral sclerosis: a clinical review. European journal of neurology, 27(10), 1918–1929. https://doi.org/10.1111/ene.14393

Mathis, S., Goizet, C., Soulages, A., Vallat, J. M., & Masson, G. L. (2019). Genetics of amyotrophic lateral sclerosis: A review. Journal of the neurological sciences, 399, 217–226. https://doi.org/10.1016/j.jns.2019.02.030

Mejzini, R., Flynn, L. L., Pitout, I. L., Fletcher, S., Wilton, S. D., & Akkari, P. A. (2019). ALS Genetics, Mechanisms, and Therapeutics: Where Are We Now?. Frontiers in neuroscience, 13, 1310. https://doi.org/10.3389/fnins.2019.01310

Moustaqim-Barrette, A., Lin, Y. Q., Pradhan, S., Neely, G. G., Bellen, H. J., & Tsuda, H. (2014). The amyotrophic lateral sclerosis 8 protein, VAP, is required for ER protein quality control. *Human molecular genetics*, *23*(8), 1975–1989. https://doi.org/10.1093/hmg/ddt594

Nishimura, A. L., Al-Chalabi, A., & Zatz, M. (2005). A common founder for amyotrophic lateral sclerosis type 8 (ALS8) in the Brazilian population. Human genetiCS, 118(3-4), 499–500. https://doi.org/10.1007/s00439-005-0031-y

Nishimura, A. L., Mitne-Neto, M., Silva, H. C., Richieri-Costa, A., Middleton, S., Cascio, D., Kok, F., Oliveira, J. R., Gillingwater, T., Webb, J., Skehel, P., & Zatz, M. (2004). A mutation in the vesicle-trafficking protein VAPB causes late-onset spinal muscular atrophy and amyotrophic lateral sclerosis. American journal of human genetiCS, 75(5), 822–831. https://doi.org/10.1086/425287

Pennetta, G., Hiesinger, P. R., Fabian-Fine, R., Meinertzhagen, I. A., & Bellen, H. J. (2002). Drosophila VAP-33A directs bouton formation at neuromuscular junctions in a dosage-dependent manner. *Neuron*, *35*(2), 291–306. https://doi.org/10.1016/s0896-6273(02)00769-9

Talbott, E. O., Malek, A. M., & Lacomis, D. (2016). The epidemiology of amyotrophic lateral sclerosis. Handbook of clinical neurology, 138, 225–238. https://doi.org/10.1016/B978-0-12-802973-2.00013-6

Tataroglu, O., & Emery, P. (2014). Studying circadian rhythms in Drosophila melanogaster. Methods (San Diego, Calif.), 68(1), 140–150. https://doi.org/10.1016/j.ymeth.2014.01.001

Tendulkar, S., Hegde, S., Thulasidharan, A., Garg, L., Kaduskar, B., Ratnaparkhi, A., Ratnaparkhi, G. S. (2022). Caspar, an adapter for VAP and TER94 delays progression of disease by regulating glial inflammation in a *Drosophila* model of ALS

Tsuda, H., Han, S. M., Yang, Y., Tong, C., Lin, Y. Q., Mohan, K., Haueter, C., Zoghbi, A., Harati, Y., Kwan, J., Miller, M. A., & Bellen, H. J. (2008). The amyotrophic lateral sclerosis 8 protein VAPB is cleaved, secreted, and acts as a ligand for Eph receptors. Cell, 133(6), 963–977. https://doi.org/10.1016/j.cell.2008.04.039

Weisskopf, M. G., Morozova, N., O'Reilly, E. J., McCullough, M. L., Calle, E. E., Thun, M. J., & Ascherio, A. (2009). Prospective study of chemical exposures and amyotrophic lateral sclerosis. Journal of neurology, neurosurgery, and psychiatry, 80(5), 558–561. https://doi.org/10.1136/jnnp.2008.156976

Wijesekera, L. C., & Leigh, P. N. (2009). Amyotrophic lateral sclerosis. Orphanet journal of rare diseases, 4, 3. https://doi.org/10.1186/1750-1172-4-3

Zarei, S., Carr, K., Reiley, L., Diaz, K., Guerra, O., Altamirano, P. F., Pagani, W., Lodin, D., Orozco, G., & Chinea, A. (2015). A comprehensive review of amyotrophic lateral sclerosis. Surgical neurology international, 6, 171. https://doi.org/10.4103/2152-7806.169561